Neutrinos for the Earth: Neutrino Oscillation Tomography of the Earth

S. T. Petcov

INFN/SISSA, Trieste, Italy,
Kavli IPMU, University of Tokyo, Japan, and
INRNE, Bulgarian Academy of Sciences, Sofia, Bulgaria

International Workshop on Neutrino Geoscience
Sun Yat-sen University
Zhuhai, China
November 16 - 18, 2026

Neutrino Tomography of the Earth is one of the most interesting, important and not yet fully explored field of reserach in today's Neutrino Physics.

Two very different methods:
neutrino absorption tomography and neutrino oscillation tomography.

This talk: Neutrino Oscillation Tomography of the Earth.

Can be done with atmospheric, solar and SN neutrinos, in principle.
At present, neutrino oscillation tomography of the Earth with atmospheric neutrino seems to be the most feasible in view of the existing and upcoming/planned adequate experiments (KM3NeT-ORCA, IceCube-DeepCore, IceCube Upgrade, HK, DUNE, possibly with JUNO, INO).

Reference Model: 3-ν mixing

$$\nu_{l\mathsf{L}} = \sum_{j=1}^{3} U_{lj}\,\nu_{j\mathsf{L}} \qquad l = e, \mu, \tau.$$

The PMNS matrix U - 3×3 unitary.

ν_j, $m_j \neq 0$: Dirac or Majorana particles.

3-ν mixing: 3-flavour neutrino oscillations possible.

ν_μ, E; at distance L: $P(\nu_\mu \to \nu_{\tau(e)}) \neq 0$, $P(\nu_\mu \to \nu_\mu) < 1$

$P(\nu_l \to \nu_{l'}) = P(\nu_l \to \nu_{l'}; E, L; U; m^2_2 - m^2_1, m^2_3 - m^2_1; N_e)$

Three Neutrino Mixing

$$\nu_{l\mathrm{L}} = \sum_{j=1}^{3} U_{lj}\, \nu_{j\mathrm{L}} \ .$$

U is the Pontecorvo-Maki-Nakagawa-Sakata (PMNS) neutrino mixing matrix,

$$U = \begin{pmatrix} U_{e1} & U_{e2} & U_{e3} \\ U_{\mu 1} & U_{\mu 2} & U_{\mu 3} \\ U_{\tau 1} & U_{\tau 2} & U_{\tau 3} \end{pmatrix}$$

- U - $n \times n$ unitary:

n	2	3	4
mixing angles: $\frac{1}{2}n(n-1)$	1	3	6

CP-violating phases:

• ν_j- Dirac:	$\frac{1}{2}(n-1)(n-2)$	0	1	3
• ν_j- Majorana:	$\frac{1}{2}n(n-1)$	1	3	6

$n = 3$: 1 Dirac and
2 additional CP-violating phases, Majorana phases

S.M. Bilenky, J. Hosek, S.T.P., 1980

PMNS Matrix: Standard Parametrization

$$U = V\,P\,, \qquad P = \begin{pmatrix} 1 & 0 & 0 \\ 0 & e^{i\frac{\alpha_{21}}{2}} & 0 \\ 0 & 0 & e^{i\frac{\alpha_{31}}{2}} \end{pmatrix}\,,$$

$$V = \begin{pmatrix} c_{12}c_{13} & s_{12}c_{13} & s_{13}e^{-i\delta} \\ -s_{12}c_{23} - c_{12}s_{23}s_{13}e^{i\delta} & c_{12}c_{23} - s_{12}s_{23}s_{13}e^{i\delta} & s_{23}c_{13} \\ s_{12}s_{23} - c_{12}c_{23}s_{13}e^{i\delta} & -c_{12}s_{23} - s_{12}c_{23}s_{13}e^{i\delta} & c_{23}c_{13} \end{pmatrix}$$

- $s_{ij} \equiv \sin\theta_{ij}$, $c_{ij} \equiv \cos\theta_{ij}$, $\theta_{ij} = [0, \frac{\pi}{2}]$,
- δ - Dirac CPV phase, $\delta = [0, 2\pi]$; CP inv.: $\delta = 0, \pi, 2\pi$;
- α_{21}, α_{31} - Majorana CPV phases; CP inv.: $\alpha_{21(31)} = k(k')\pi$, $k(k') = 0, 1, 2...$

  S.M. Bilenky et al., 1980
- $\Delta m^2_{\odot} \equiv \Delta m^2_{21} \cong 7.34 \times 10^{-5}$ eV$^2 > 0$, $\sin^2\theta_{12} \cong 0.305$, $\cos 2\theta_{12} \gtrsim 0.306$ (3σ),
- $|\Delta m^2_{31(32)}| \cong 2.448\ (2.502) \times 10^{-3}$ eV^2, $\sin^2\theta_{23} \cong 0.545\ (0.551)$, NO (IO) ,
- θ_{13} - the CHOOZ angle: $\sin^2\theta_{13} = 0.0222\ (0.0223)$

  F. Capozzi et al. (Bari Group), arXiv:2003.08511.

- $\mathrm{sgn}(\Delta m^2_{\mathrm{atm}}) = \mathrm{sgn}(\Delta m^2_{31(32)})$ not determined

$$\Delta m^2_{\mathrm{atm}} \equiv \Delta m^2_{31} > 0, \quad \text{normal mass ordering (NO)}$$

$$\Delta m^2_{\mathrm{atm}} \equiv \Delta m^2_{32} < 0, \quad \text{inverted mass ordering (IO)}$$

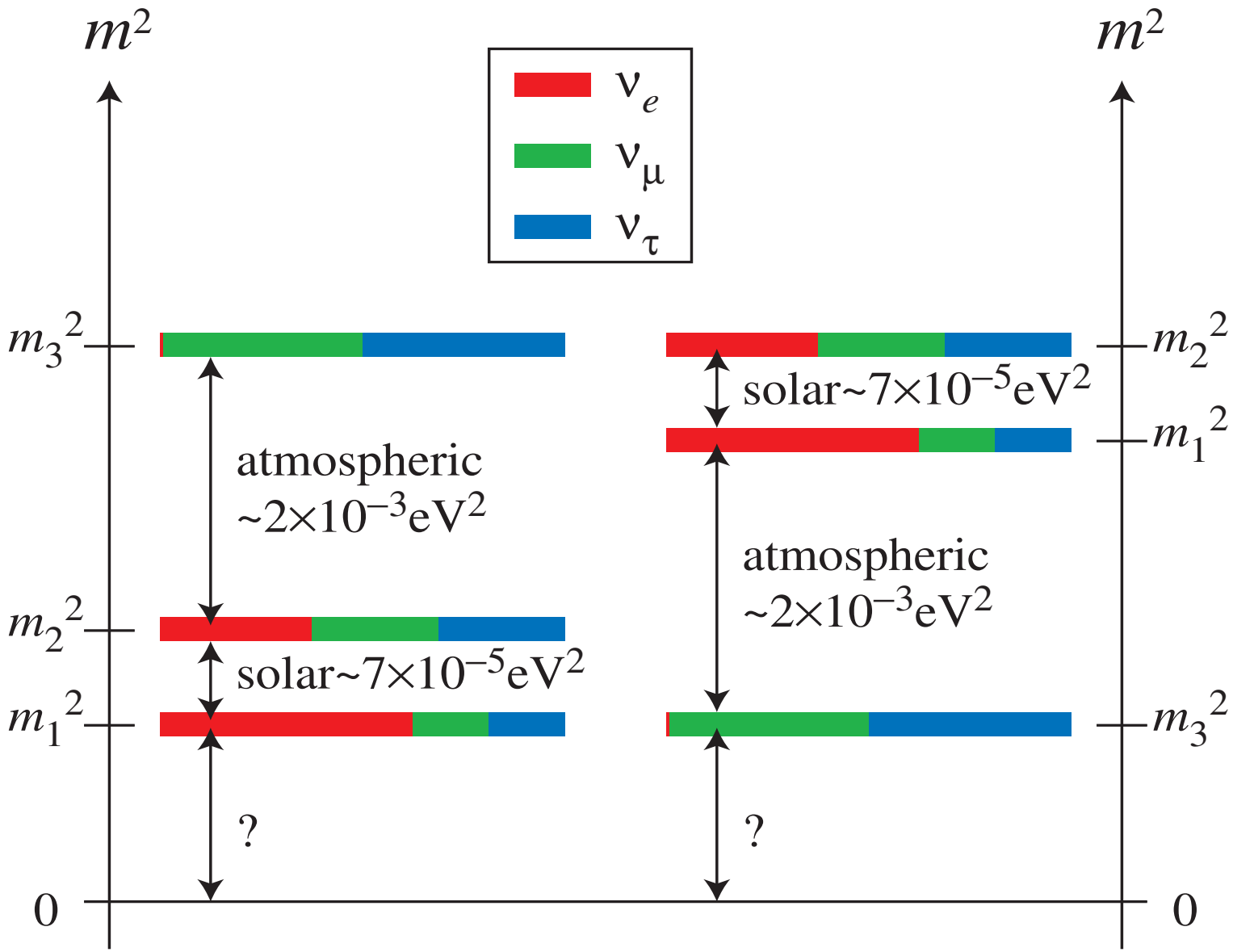
Convention: $m_1 < m_2 < m_3$ - NO, $m_3 < m_1 < m_2$ - IO

$$m_1 \ll m_2 < m_3, \qquad \text{NH},$$

$$m_3 \ll m_1 < m_2, \qquad \text{IH},$$

$$m_1 \cong m_2 \cong m_3,\ m^2_{1,2,3} >> |\Delta m^2_{31(32)}|,\ \text{QD};\ m_j \gtrsim 0.10\ \text{eV}.$$

- $m_2 = \sqrt{m_1^2 + \Delta m^2_{21}}$, $m_3 = \sqrt{m_1^2 + \Delta m^2_{31}}$ - NO;
- $m_1 = \sqrt{m_3^2 + \Delta m^2_{23} - \Delta m^2_{21}}$, $m_2 = \sqrt{m_3^2 + \Delta m^2_{23}}$ - IO;


m^2
ν_e
ν_μ
ν_τ
m_3^2
atmospheric
$\sim 2\times10^{-3}\text{eV}^2$
m_2^2
solar$\sim 7\times10^{-5}\text{eV}^2$
m_1^2
?
0
m^2
m_2^2
solar$\sim 7\times10^{-5}\text{eV}^2$
m_1^2
atmospheric
$\sim 2\times10^{-3}\text{eV}^2$
m_3^2
?
0

Parameter	Ordering	Best fit	1σ range	2σ range	3σ range	"1σ" (%)
$\Delta m^2_{21}/10^{-5}$ eV^2	NO, IO	$7.49^{+0.19}_{-0.19}$	–	–	6.92 – 8.05	–
$\sin^2\theta_{12}/10^{-1}$	NO, IO	$3.08^{+0.012}_{-0.011}$	–	–	2.75 – 3.45	–
$\Delta m^2_{31}/10^{-3}$ eV^2	NO	$2.513^{+0.021}_{-0.019}$	–	–	2.451 – 2.578	–
$\Delta m^{32}/10^{-3}$ eV^2	IO	-2.484 ± 0.020	–	–	-2.547 – (-2.421)	–
$\sin^2\theta_{13}/10^{-2}$	NO	$2.215^{+0.056}_{-0.058}$	–	–	2.0300 – 2.388	–
	IO	2.231 ± 0.056	–	–	2.060 – 2.409	–
$\sin^2\theta_{23}/10^{-1}$	NO	$4.70^{+0.017}_{-0.013}$	–	–	**4.35 – 5.85**	–
	IO	$5.50^{+0.012}_{-0.015}$	–	–	**4.40 – 5.84**	–
δ	NO	212^{+26}_{-41}	–	–	124 – 364	–
	IO	274^{+22}_{-25}	–	–	**201 – 335**	–
$\Delta\chi^2_{\text{IO}-\text{NO}}$	IO–NO	+6.1 (2.45σ)				

Global 3ν analysis of oscillation parameters: best-fit values and allowed ranges at $N_\sigma = 3$ for either NO or IO, including all data (also the SK atmospheric neutrino data). The last row reports the difference between the χ^2 minima in IO and NO. The results on the NO and CPV due to δ are inconclusive.

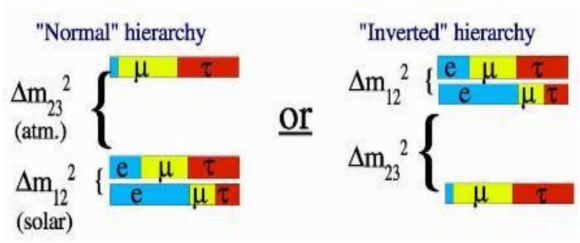
I. Esteban et al., arXiv:2410.05380 (NuFit-6.0 results).

$\sin^2\theta_{23}$ **- relatively large uncertainty.**
$\Delta m^2_{21}/|\Delta m^2_{31}| \cong 1/30$.

M. Jin, I. Martinez-Soler et al., arXiv: 2610.12208, combining data from IceCube-DeepCore, KM3NeT/ORCA, SK, JUNO find that IO is disfavored with respect to NO at 3.9σ C.L.

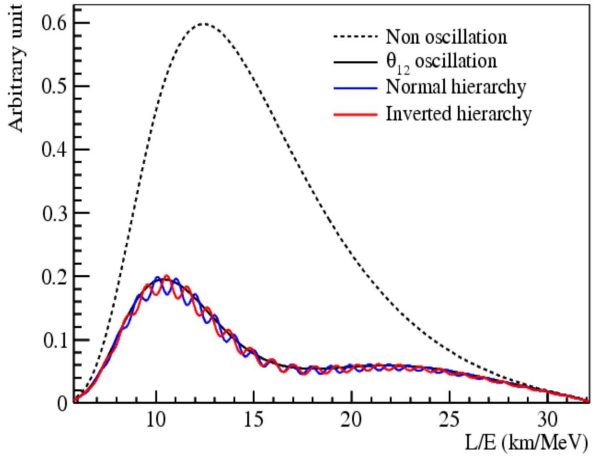

Guang Zhou
Huizhou
Dongguan
Zhaoqing
CNS
2.5 h drive
Shen Zhen
Huizhou NPP
Lufeng NPP
Daya Bay
NPP
Zhongshan
Zhu Hai
Zhujiang River Estuary
Hong Kong
Hong Kong
Macau
Macau
JUNO site
53 km
53 km
Taishan NPP
Yangjiang NPP

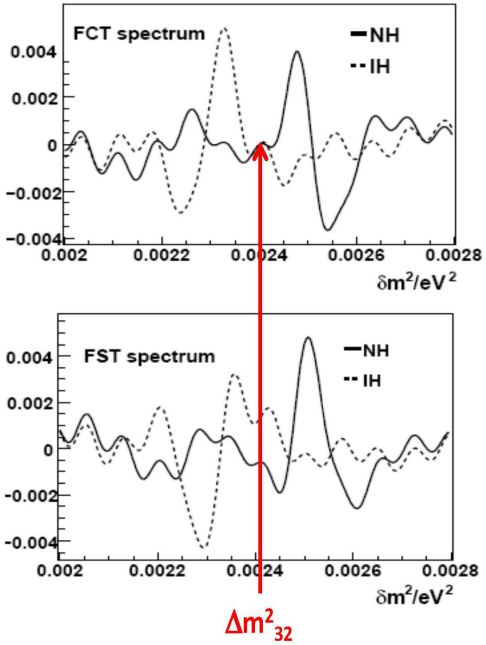
Mass Ordering by Reactor Neutrinos



$$\Delta m^2_{31} = \Delta m^2_{32} + \Delta m^2_{21}$$
$$\text{NH}: |\Delta m^2_{31}| = |\Delta m^2_{32}| + |\Delta m^2_{21}|$$
$$\text{IH}: |\Delta m^2_{31}| = |\Delta m^2_{32}| - |\Delta m^2_{21}|$$

$\frac{\Delta m^2_{21}}{|\Delta m^2_{32}|} \sim 3\%$

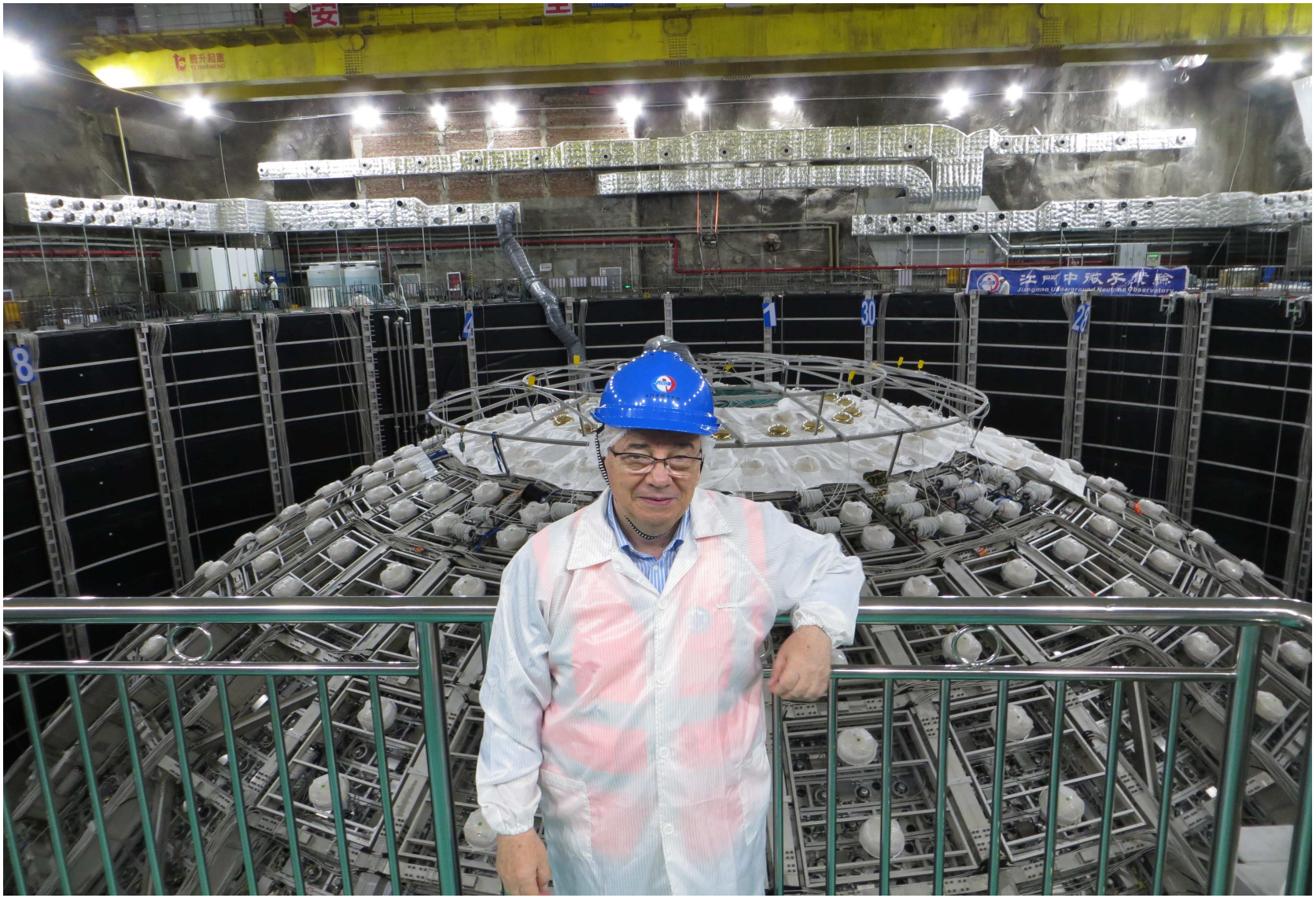




$$P_{ee}(L/E) = 1 - P_{21} - P_{31} - P_{32}$$
$$P_{21} = \cos^4(\theta_{13})\sin^2(2\theta_{12})\sin^2(\Delta_{21})$$
$$P_{31} = \cos^2(\theta_{12})\sin^2(2\theta_{13})\sin^2(\Delta_{31})$$
$$P_{32} = \sin^2(\theta_{12})\sin^2(2\theta_{13})\sin^2(\Delta_{32})$$

S. Petcov and Piai, Phys. Lett. B 553, 94-106(2002)
J. Learned et al., PRD 78(2008)071302
L. Zhan, YFW et al., PRD 78(2008)111103

Y. Wang, talk given at CERN on March 20, 2024


江门中微子实验
Jiangmen Underground Neutrino Observatory

JUNO started taking physics data on August 26, 2025. The first results were released on November 11, 2025 (after 59.1 days); new results were reported at the Neutrino 2026 Conference:

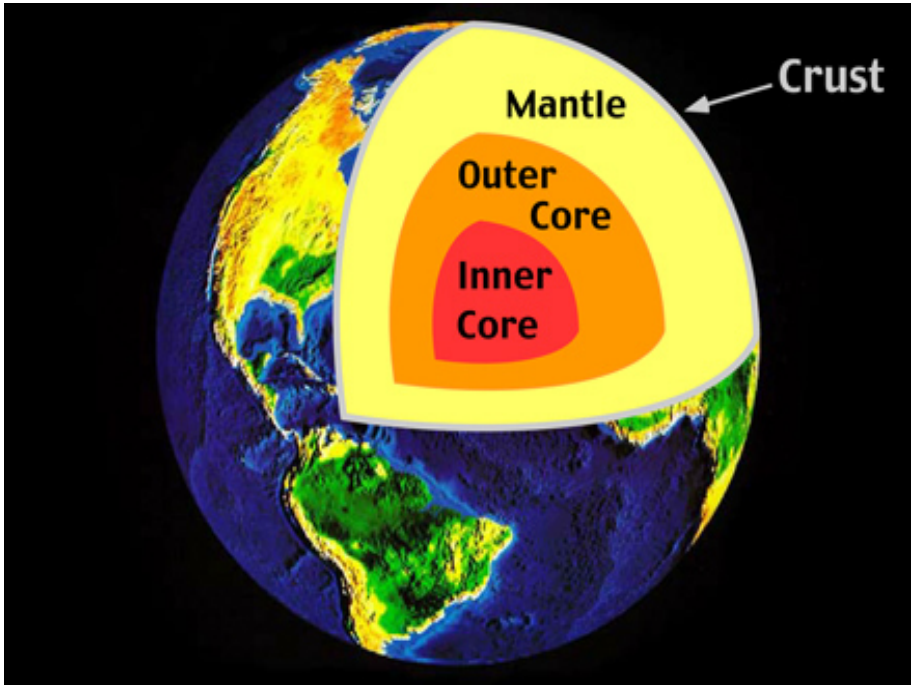
$\sin^2\theta_{12} = 0.3036 \pm 0.0064$,
$\Delta m^2_{21} = (7.388 \pm 0.078) \times 10^{-5}$ eV^2

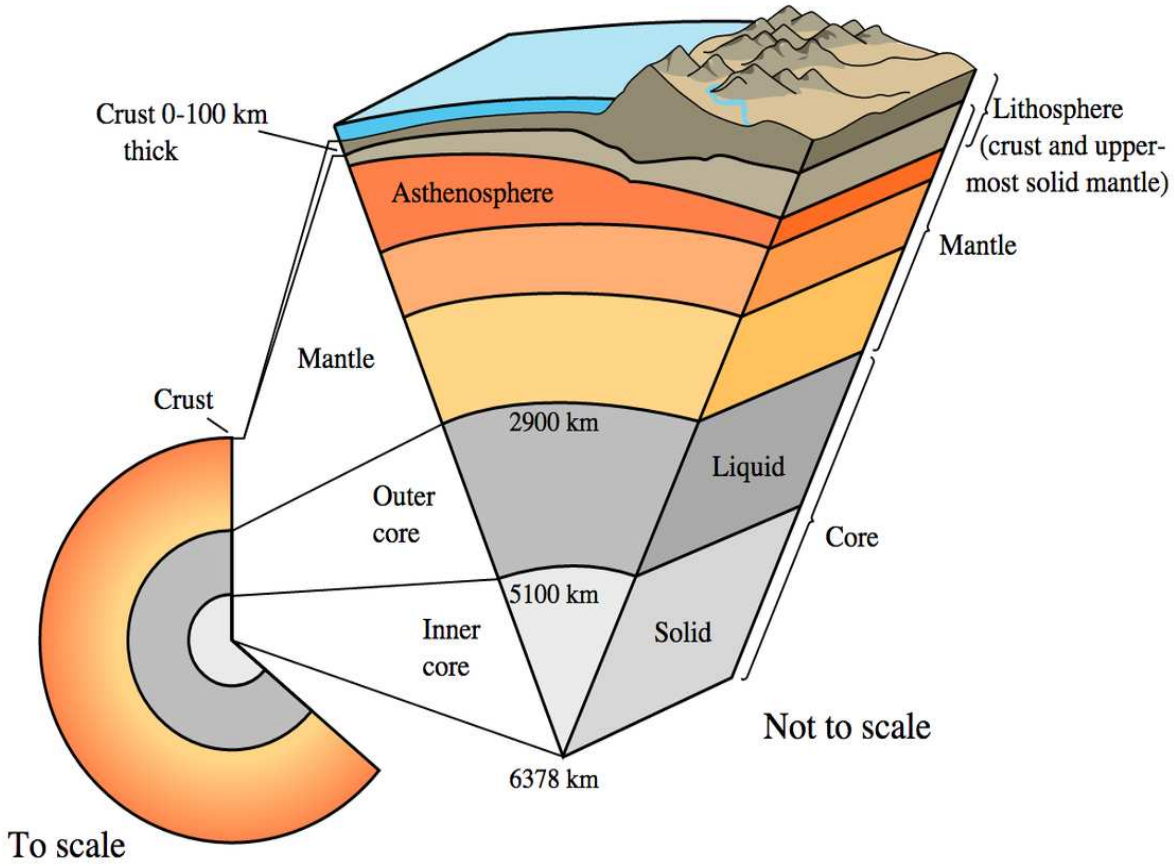
Improvemed by a factor of approximately 1.8 (2.6) the precision on $\sin^2\theta_{12}$ (Δm^2_{12}).

$|\Delta m^2_{31}|$ measured with 1σ error of 1%.

These impressive results have a large number of important implications; they are relevant for performing neutrino oscillation tomography of the Earth reducing the uncertainties due to the oscillation parameters (the precision on $\sin^2\theta_{12}$, Δm^2_{21} - particularly relevant for the oscillation tomography with the DUNE detector).

The Earth




Crust 0-100 km
thick
Asthenosphere
Lithosphere
(crust and upper-
most solid mantle)
Mantle
Mantle
Crust
2900 km
Liquid
Outer
core
Core
5100 km
Inner
core
Solid
Not to scale
6378 km
To scale

At present our knowledge about the interior composition of the Earth and its density structure is based primarily on seismological and geophysical data.

See, e.g., W.F. McDonough, "Treatise on Geochemistry: The Mantle and Core", vol. 2 (ed. R. W. Carlson, Elsevier-Pergamon, Oxford, 2003), p. 547.
B.L.N. Kennett, Geophys. J. Int. **132**, 374 (1998);
G. Masters and D. Gubbins, Phys. Earth Planet. Inter. **140**, 159 (2003).

These data were used to construct the Preliminary Reference Earth Model (PREM) of the density distribution of the Earth: A. M. Dziewonski and D. L. Anderson, "Preliminary reference earth model," Phys. Earth Planet. Interiors 25 (1981) 297.

In the PREM model, $\rho_{\rm E}$ is assumed to be spherically symmetric, $\rho_{\rm E} = \rho_{\rm E}(r)$, r being the distance from the Earth center, and there are three major density structures - the inner core, the outer core and the mantle, and a certain number of substructures (shells or layers). The mantle has five shells in the model. There are three "thin" layers close to the Earth surface: the ocean and the two crust layers (total width ~ 100 km).

The change of $\rho_{\rm E}$ (N_e) from the mantle to the core and from the outer core to the inner core, according to PREM, can well be approximated by the step function.

The Earth (PREM)

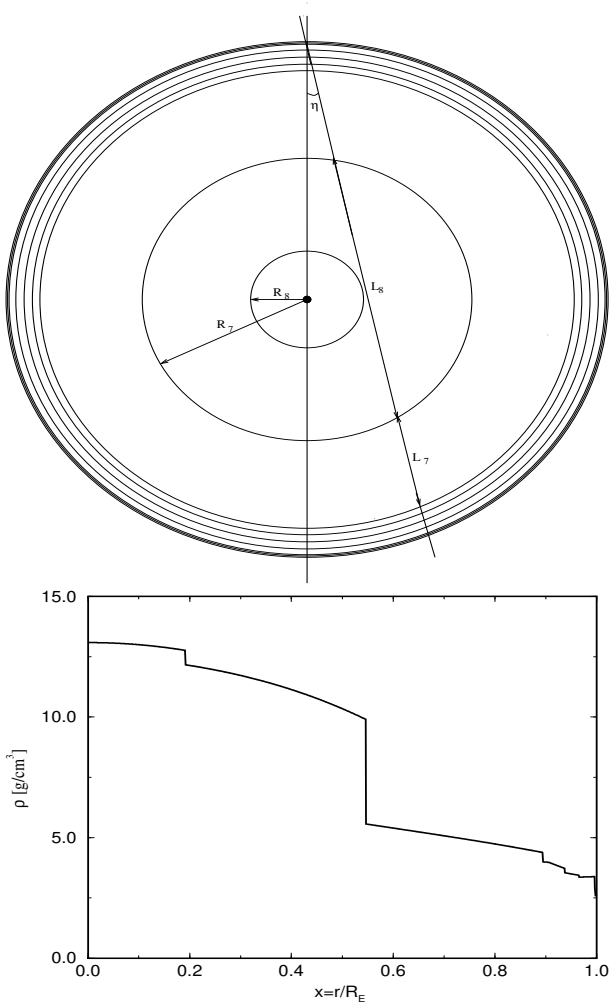


FIG. 1. Density profile of the Earth.

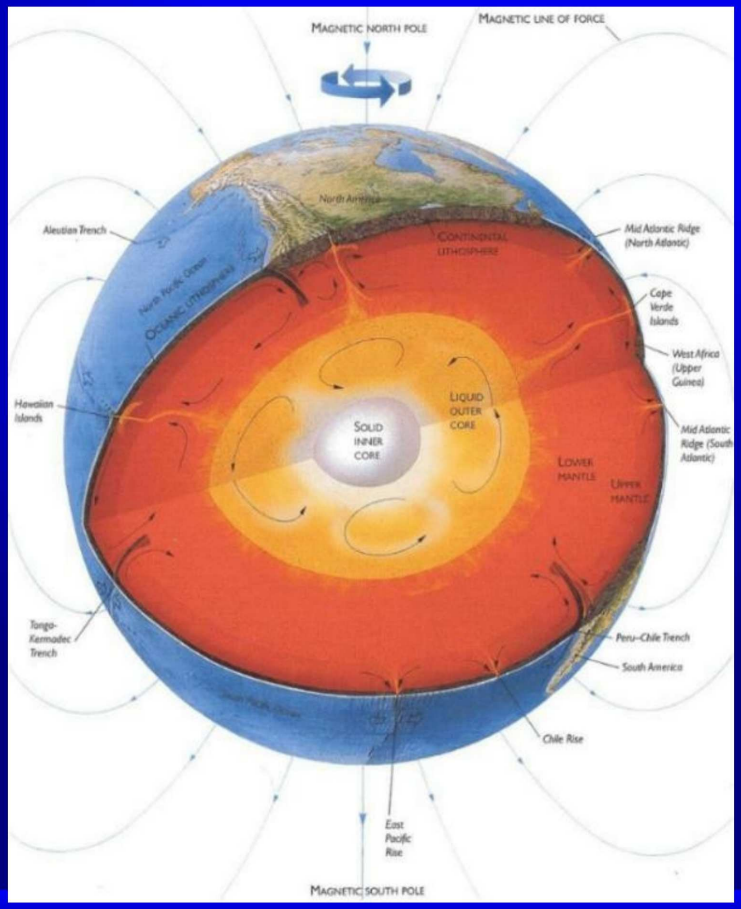
$R_\oplus = 6371$ km; $R_{\rm IC} = 1221.5$ km; $R_{\rm C} = 3480$ km; $D_{\rm man} = 2891$ km;
$\bar{\rho}_{\rm man} = 4.45$ g/cm^3; $\bar{\rho}_{\rm C} = 10.99$ g/cm^3; $\bar{\rho}_{\rm IC} = 12.89$ g/cm^3; $\bar{\rho}_{\rm OC} = 10.90$ g/cm^3.

PREM: good/useful "Reference" model; $\rho_{\rm E}^{\rm PREM}(\mathrm{r}) = \rho_{\rm E}^{\rm PREM}(r)$, in particular. Used in practically all studies of ν tomography of the Earth.

Future: more sophisticated $\rho_{\rm E}(\mathrm{r})$ suggested by geophysics/seismology can/should be used.

The formalism of using 3-dimensional Earth density distribution $\rho_{\rm E}(\mathrm{r})$ in neutrino tomography of the Earth studies was developed in J. Wei, J. Xing, S. Lin, X. Li and J. Tian, Chinese Physics C (2026) 073104.

Earth's Core



OUTER CORE

- *fluid (viscosity similar to water)*
- *radius of 3480 km (bigger than Mars)*
- *~90% Fe/Ni, 10% (Si, S, ??)*

INNER CORE

- *solid-ish (viscosity of $10^{10\text{-}20}$ Pas, Possion's ratio of 0.42)*
- *radius of 1221 km (bigger than Pluto)*
- *~95% Fe/Ni, 5% (Si,S,??)*
- *elastically anisotropic (conductively too ??)*
- *May be rotating faster or slower than the rest of the Earth*

K.D. Koper, talk at the MMTE 2022 workshop (Snowbird, Utah)

Mantle: 44.8% Oxigen, 21.5% Silicon, 22.8% Magnesium + iron, aluminum, calcium, sodium and potassium - all bound together in silicate rocks (in the form of oxides).

Spherically symmetric ρ_{E}: the ν trajectory through the Earth is specified by the nadir (zenith) angle θ_n (or θ_z).

For $\theta_n \leq 33.17^o$, or path lengths $L \geq 10660$ km, neutrinos cross the Earth core.

The path length for neutrinos which cross only the Earth mantle is given by $L = 2R_\oplus \cos\theta_n$, θ_n.

If neutrinos cross the Earth core, the lengths of the paths in the mantle, $2L^{\mathsf{man}}$, and in the core, L^{core}, are determined by: $L^{\mathsf{man}} = R_\oplus \cos\theta_n - (R_c^2 - R_\oplus^2 \sin^2\theta_n)^{\frac{1}{2}}$, $L^{\mathsf{core}} = 2(R_c^2 - R_\oplus^2 \sin^2\theta_n)^{\frac{1}{2}}$.

$\rho_{\mathsf{E}}(r)$ (N_e) changes relatively little around the quoted mean values along the trajectories of neutrinos which cross a substantial part of the Earth mantle, or the mantle and the outer core, or the mantle and the outer core and the inner core.

The determination of the radial density distributions in the mantle and core, $\rho_{man}(r)$ and $\rho_c(r)$, from seismological and geophysical data is not direct and suffers from uncertainties. It is difficult to quantify these uncertainties.

B. A. Bolt, Q. J. R. Astron. Soc. **32**, 367 (1991).
B.L.N. Kennett, Geophys. J. Int. **132**, 374 (1998);
G. Masters and D. Gubbins, Phys. Earth Planet. Inter. **140**, 159 (2003).

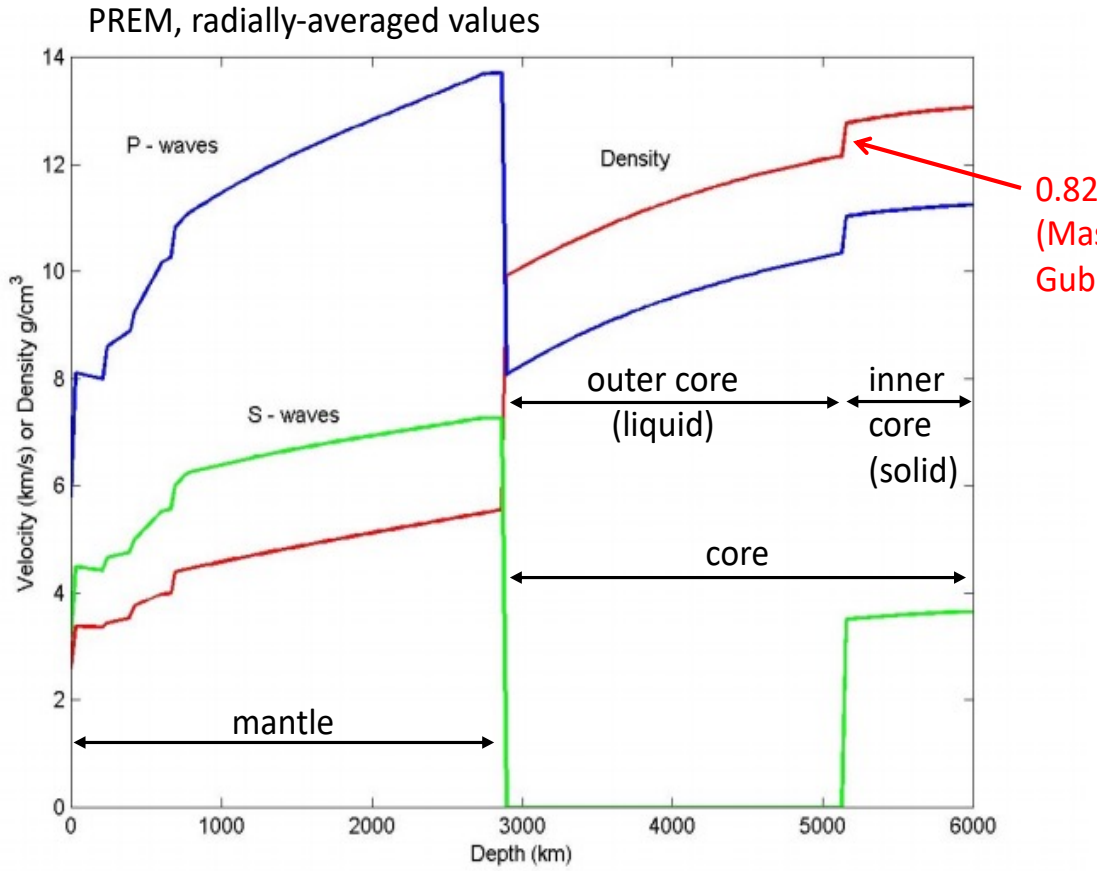
It requires the knowledge, in particular, of the seismic wave speed velosity distribution in the interrior of the Earth, which depends on the pressure, tempertaure, composition and elastic properties of the Earth's interior that are not known with a good/high precision.
Often $\rho_{\rm E}(r)$ is determined using an empirical relation between the seismic wave velosities and $\rho_{\rm E}(r)$ (one example is the Birch low, which may fail at the higher densities of the core) and the so-called "Adams-Williamson eqaution" (from 1923). E. Williamson and L.H. Adams, J. Wash. Acad. Sci. 13 (1923) 413.

The most prcise determination of $\rho_{\rm E}(r)$ seems to be achieved by using the data on the low frequency (0.2-10 mHz) normal mode oscillations of the Earth surface following relatively strong earhquakes ($M_w \sim (8-9)$).

A. Deuss, talk at MMTE 2023, Paris, France

An approximate and perhaps rather conservative estimate of this uncertainty for $\rho_{\rm man}(r)$ is $\sim 5\%$; for the core density $\rho_c(r)$ it is larger and can be significantly larger (Bolt:1991,Kennett:1998,Masters:2003).

Density Structure



0.82+/-0.18 g/cc
(Masters &
Gubbins 2003)

F. Nimmo, talk at the MMTE 2022 workshop (Snowbird, Utah)

A precise knowledge of $\rho_{\mathrm{E}}(r)$ and of $\bar{\rho}_{\mathrm{man}}$, $\bar{\rho}_{\mathrm{C}}$ and $\bar{\rho}_{\mathrm{IC}}$, is essential for understanding the physical conditions and fundamental aspects of the structure and properties of the Earth's interior
(including the dynamics of mantle and core,
the bulk composition of the Earth's three structures,
the generation, properties and evolution of the Earth's magnetic field and the gravity field of the Earth)
(Bolt:1991,Yoder:1995,McDonough:2003,McDonough:2008zz).

The thermal evolution of the Earth's core, in particular, depends critically on the density change across the inner core - outer core boundary (see, e.g., Baffet:1991).

An independent determination of $\rho_{\mathrm{E}}(r)$ and of $\bar{\rho}_{\mathrm{man}}$, $\bar{\rho}_{\mathrm{C}}$ and $\bar{\rho}_{\mathrm{IC}}$, is highly desirable and would be extremely useful.

A unique alternative method of determination of the density profile of the Earth is the neutrino tomography of the Earth.

The propagation of the active flavour neutrinos and antineutrinos ν_α and $\bar{\nu}_\alpha$, $\alpha = e, \mu, \tau$, in the Earth is affected by the Earth matter.

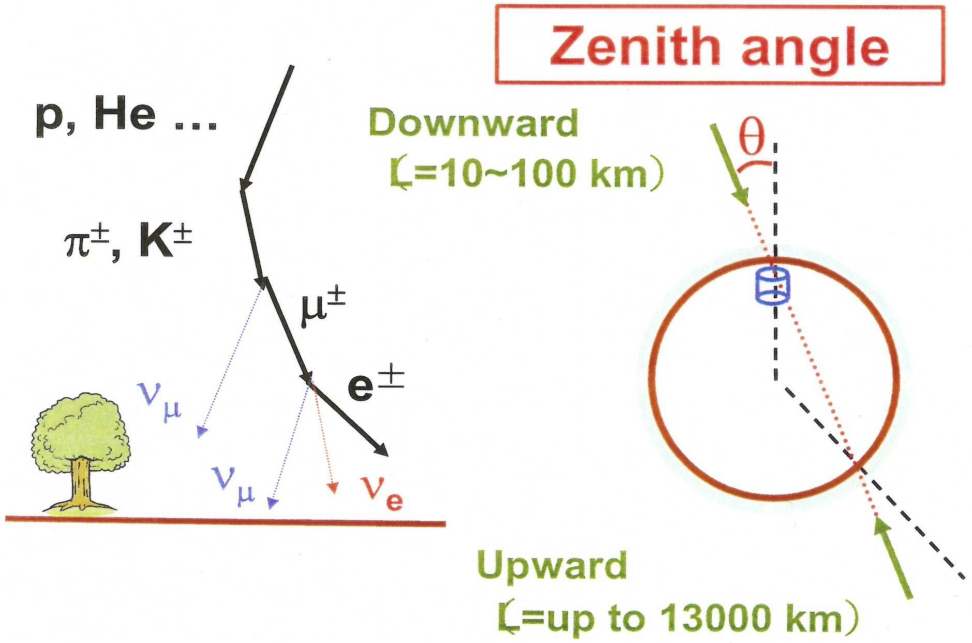
The original idea is based on the observation that
$\sigma(\nu_\alpha(\bar{\nu}_\alpha) + N)$ rises with energy.
For ν_α, $\bar{\nu}_\alpha$ with $E_\nu \gtrsim$ a few TeV, the inelastic scattering off protons and neutrons leads to absorption of νs and thus to attenuation of the initial ν flux.
The magnitude of the attenuation depends on the Earth matter density profile along the neutrino path.
Attenuation data for νs with different path-lengths in the Earth carry information about the matter density distribution in the Earth interior.
The absorption method of Earth tomography with accelerator neutrino beams, which is difficult (if not impossible) to realise in practice , was discussed first by Placci and Zavattini in 1973 and Volkova and Zatsepin in 1974, and later in grater detail in Nedyalkov:1981, Nedyalkov:1981yy, Nedyalkov:1982, Nedyalkov:1983, DeRujula:1983ya, Wilson:1983an, Askar:1984, Borisov:1986sm, Borisov:1989kh, Winter:2006vg, Kuo95, Jain:1999kp, Reynoso:2004dt.

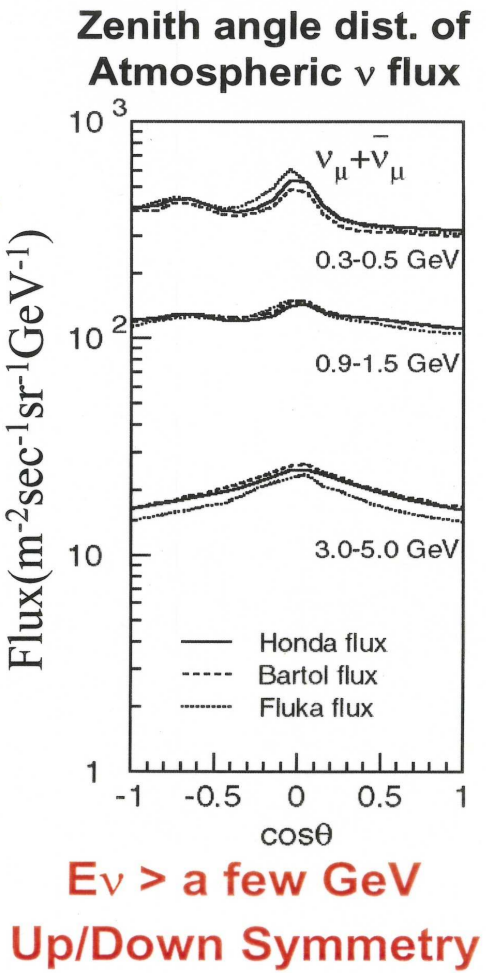
Atmospheric νs are a perfect tool for performing Earth tomography:
i) consist of significant fluxes of ν_μ, ν_e, $\bar{\nu}_\mu$ and $\bar{\nu}_e$, produced in the interactions of cosmic rays with the Earth atmosphere,
ii) have a wide range of energies spanning the interval from a few MeV to multi-GeV to multi-TeV,
iii) being produced isotropically in the upper part of the Earth atmosphere at a height of ~ 15 km, they travel distances from ~ 15 km to 12742 km before reaching detectors located on the Earth surface, crossing the Earth along all possible directions and thus "scanning" the Earth interior.

See, e.g., T.K. Gaisser and M. Honda, Ann. Rev. Nucl. Part. Sci. **52** (2002) 153 [arXiv:hep-ph/0203272]

The interaction rates that allow to get information about the Earth density distribution can be obtained in the currently taking data IceCube (including DeepCore and the Upgrade) and the gradually upgraded KM3NeT/ORCA experiments, Hyper Kamiokande (HK) and possibly in DUNE (requires detection of protons in $\nu_l + n \to l^- + p$, $l = e, \mu$, with $E_\nu \sim 200$ MeV), which are under construction, in the planned INO experiment and possibly in the JUNO experiment.

Atmospheric neutrinos



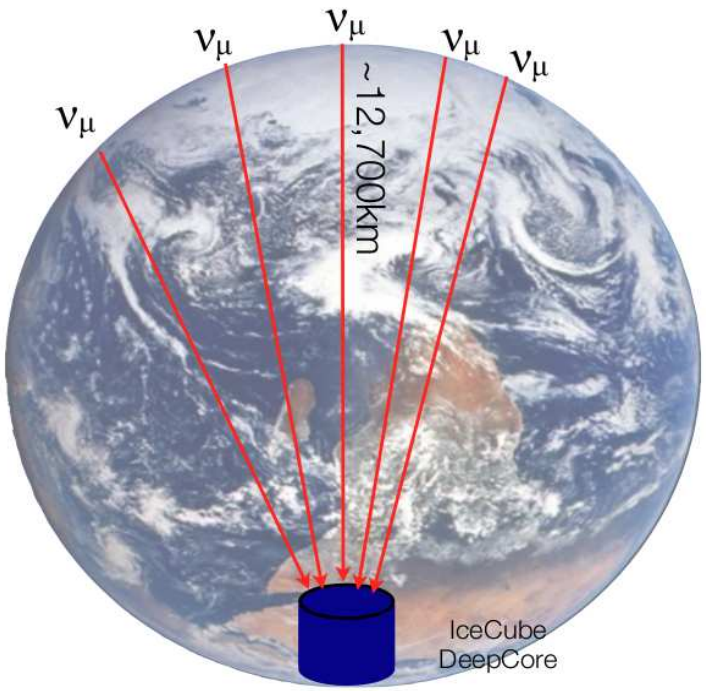


Eν > a few GeV

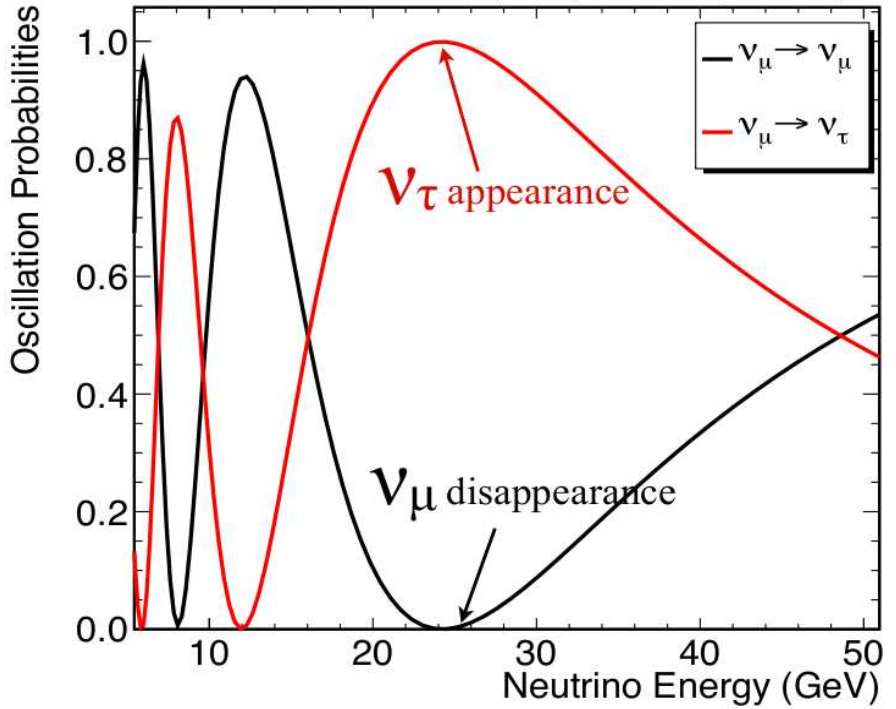
Up/Down Symmetry

Neutrino Oscillation Source

- Northern Hemisphere ν_μ oscillating over one earth radii produces ν_μ (ν_τ) oscillation minimum(maximum) at ~25 GeV
  - Covers all possible terrestrial baselines
  - "Beam" is free and never turns off



Mena, Mocioiu & Razzaque, *Phys. Rev.* D**78**, 093003 (2008)



The idea of using the absorption method of Earth tomography with atmospheric neutrinos was discussed first in
M. C. Gonzalez-Garcia, F. Halzen, M. Maltoni and H. K. M. Tanaka, Phys. Rev. Lett. 100 (2008) 061802.

A. Donini, S. Palomares-Ruiz and J. Salvado, Nature Phys. 15 (2019) 37, using the IceCube zenith angle distribution data on multi-TeV (1.5-20.0 TeV) atmospheric ν_μ and $\bar{\nu}_\mu$ obtained information about $\rho_{\mathsf{E}}(r)$, which, although not very precise, broadly agrees with the PREM model.

"Weighted" the Earth with neutrinos: $M^\nu_\oplus = (6.0^{+1.6}_{-1.3}) \times 10^{24}$ kg (1σ),
to be compared with the gravitationally determined value:
$M_\oplus = (5.9722 \pm 0.0006) \times 10^{24}$ kg.
Found $\bar{\rho}_{\mathsf{C}} - \bar{\rho}_{\mathsf{man}} = 13.1^{+6.3}_{-5.8}$ g/cm^3.

Marked the beginning of real experimental data driven neutrino tomography of the Earth.

In R. Abassi *et al.*, arXiv:2510.09763, the IceCube collaboration, using data accumulated over 11 years in the energy interval 500 GeV - 100 TeV presented a more prcise determination (by approximately by a factor ~ 1.4) of $M^\nu_\oplus$ with $M^\nu_{\oplus,mean} = 6.249 \times 10^{24}$ kg.

Neutrino oscillation Earth tomography is based on the fact that given the measured $3-\nu$ oscillation parameters

Δm^2_{21}, $|\Delta m^2_{31}|$, $\sin^2\theta_{12}$, $\sin^2\theta_{13}$, $\sin^2\theta_{23}$,

for $E_\nu \sim (2-10)$ GeV ($E_\nu \sim 0.2$ GeV, DUNE),

$P_{3\nu}(\nu_{\mu(e)} \to \nu_{e(\mu)})$ or $P_{3\nu}(\bar{\nu}_{\mu(e)} \to \bar{\nu}_{e(\mu)})$

exhibits a strong dependence on $\rho_E(r)$ along the ν path in the Earth via

$$V_{eff} = \pm\sqrt{2}\,G_F\,N_e(r) = \pm\sqrt{2}\,G_F Y_e \frac{\rho_E(r)}{m_N}\,,$$

$$Y_e = \frac{N_e(r)}{N_p(r)+N_n(r)}\,,$$ "+": $\nu_{\mu(e)} \to \nu_{e(\mu)}$; "-": $\bar{\nu}_{\mu(e)} \to \bar{\nu}_{e(\mu)}$.

Isotopically symmetric medium: $N_e(r) = N_p(r) = N_n(r)$: $Y_e = 0.5$.

$\mathrm{sgn}(\Delta m^2_{31})$ **– not yet determined from data.**

$\Delta m^2_{31} > 0$ **(NO):** $P_{3\nu}(\nu_{\mu(e)} \to \nu_{e(\mu)})$ **– resonantly enhanced,** $P_{3\nu}(\bar{\nu}_{\mu(e)} \to \bar{\nu}_{e(\mu)})$ **– suppressed.**

$\Delta m^2_{31} < 0$ **(IO):** $P_{3\nu}(\nu_{\mu(e)} \to \nu_{e(\mu)})$ **– suppressed,** $P_{3\nu}(\bar{\nu}_{\mu(e)} \to \bar{\nu}_{e(\mu)})$ **– resonantly enhanced.**

The neutrino oscillation method is sensitive to changes of $\rho_E(r)$ over scales $L \gtrsim L_{\rm osc}/(2\pi)$. In the cases of interest $L_{\rm osc}/(2\pi) \sim (0.5 - 1.0) \times 10^3$ km. Thus, very "fine" structures in $\rho_E(r)$ are difficult to "resolve".

There is a strong dependence of the results on $\sin^2\theta_{23}$
(not precisely measured yet, $\sin^2\theta_{23} = (0.43 - 0.58)$ allowed at 3σ)
and on the currently still undetermined neutrino mass ordering (NO or IO), although the existing data favors NO.

$\sin^2\theta_{23}$: T2K, NOνA, T2HK, DUNE

Neutrino mass ordering (NO or IO): JUNO, ORCA, DUNE, T2HK + HK(atm. ν data).

JUNO began physics runs at the end of August, 2025.

M. Jin et al., arXiv: 2610.12208, combining data from IceCube-DeepCore, KM3NeT/ORCA, SK, JUNO find that IO is disfavored with respect to NO at 3.9σ C.L. (at 3.3σ C.L. without JUNO data).

HK is under construction and is scheduled to start data-taking in 2028.

DUNE is also under construction.

For $E_\nu \sim (2 - 10)$ **GeV**, effects of Δm^2_{21}, θ_{12} and $\delta_{\rm CP}$ – sub-leading.

$E_\nu \sim 0.2$ GeV (DUNE), Δm^2_{31} "averaged out".

Atmospheric ν experiments (ORCA, IceCube, HK, INO, DUNE)

Of interest: $\nu_{\mu(e)} \to \nu_{e(\mu)}$, $\bar{\nu}_{\mu(e)} \to \bar{\nu}_{e(\mu)}$ oscillations in the Earth ($E_\nu \gtrsim 2$ GeV).

$$P_{3\nu}(\nu_e \to \nu_\mu) \cong P_{3\nu}(\nu_\mu \to \nu_e) \cong s^2_{23}\, P_{2\nu}\,, P_{3\nu}(\nu_e \to \nu_\tau) \cong c^2_{23}\, P_{2\nu}\,,$$
$$P_{3\nu}(\nu_\mu \to \nu_\mu) \cong 1 - s^4_{23}\; P_{2\nu} - 2c^2_{23}s^2_{23}\; \left[1 - Re\; (e^{-i\kappa} A_{2\nu}(\nu_\tau \to \nu_\tau))\right]\,,$$

$P_{2\nu} \equiv P_{2\nu}(\Delta m^2_{31}, \theta_{13}; E, \theta_n; N_e)$: 2-$\nu$ $\nu_e \to \nu'_\tau$ oscillations in the Earth,
$\nu'_\tau = s_{23}\,\nu_\mu + c_{23}\,\nu_\tau$; $\Delta m^2_{21} \ll |\Delta m^2_{31(32)}|$, $E_\nu \gtrsim 2$ GeV;

κ and $A_{2\nu}(\nu_\tau \to \nu_\tau) \equiv A_{2\nu}$ are known phase and 2-ν amplitude.

NO: $\nu_{\mu(e)} \to \nu_{e(\mu)}$ matter enhanced, $\bar{\nu}_{\mu(e)} \to \bar{\nu}_{e(\mu)}$ - suppressed

IO: $\bar{\nu}_{\mu(e)} \to \bar{\nu}_{e(\mu)}$ matter enhanced, $\nu_{\mu(e)} \to \nu_{e(\mu)}$–suppressed

No charge identification (IceCube, KM3NeT-ORCA, HK(?)); event rate (DIS regime): $[2\sigma(\nu_l + N \to l^- + X) + \sigma(\bar{\nu}_l + N \to l^+ + X)]/3$

Charge identification: INO, DUNE; event rate (DIS regime):
$\sigma(\nu_l + N \to l^- + X)$, $\sigma(\bar{\nu}_l + N \to l^+ + X)$

$E_\nu \sim 200$ MeV (DUNE): $P_{3\nu}(\nu_e \to \nu_\mu) \cong P_{3\nu}(\nu_\mu \to \nu_e) \cong \cos^2\theta_{23}\, \tilde{P}_{2\nu}$,
$\tilde{P}_{2\nu} \equiv P_{2\nu}(\Delta m^2_{21}, \theta_{12}; E, \theta_n; N_e)$: 2-$\nu$ $\nu_e \to \tilde{\nu}'_\tau$ oscillations in the Earth,
$\tilde{\nu}'_\tau = c_{23}\,\nu_\mu - s_{23}\,\nu_\tau$; $\nu_l + n \to l^- + p$, $l = e, \mu$; ET: E_p, θ_p.

All detectors: strong dependence on $\sin^2\theta_{23}$ and on neutrino MO.

The oscillations $\nu_\alpha \leftrightarrow \nu_\beta$ and $\bar{\nu}_\alpha \leftrightarrow \bar{\nu}_\beta$, $\alpha, \beta = e, \mu$, having $E \sim (0.1 - 15.0)$ GeV and traversing the Earth can be strongly modified by the Earth matter effects. These modifications depend on the Earth matter density (more precisely, the electron number density $N_e(r)$, see further) along the path of the νs. Thus, by studying the effects of Earth matter on the oscillations of, e.g., ν_μ and ν_e ($\bar{\nu}_\mu$ and $\bar{\nu}_e$) neutrinos traversing the Earth along different trajectories it is possible to obtain information about the Earth (electron number) density distribution.

Neutrino Oscillations in Matter (Earth mantle)

When neutrinos propagate in matter, they interact with the backgrpound of electrons, protons and neutrnos, which generates an effective potential in the neutrino Hamiltonian: $H = H_{vac} + V_{eff}$.

This modifies the neutrino mixing since the eigenstates and the eigenvalues of H_{vac} **and of** $H = H_{vac} + V_{eff}$ **are different, leading to a different oscillation probability w.r.t to that in vacuum.**

Typically the matter background is not CP and CPT symmetric, e.g., the Earth and the Sun contain only electrons, protons and neutrons, and the resulting oscillations violate CP and CPT symmetries.

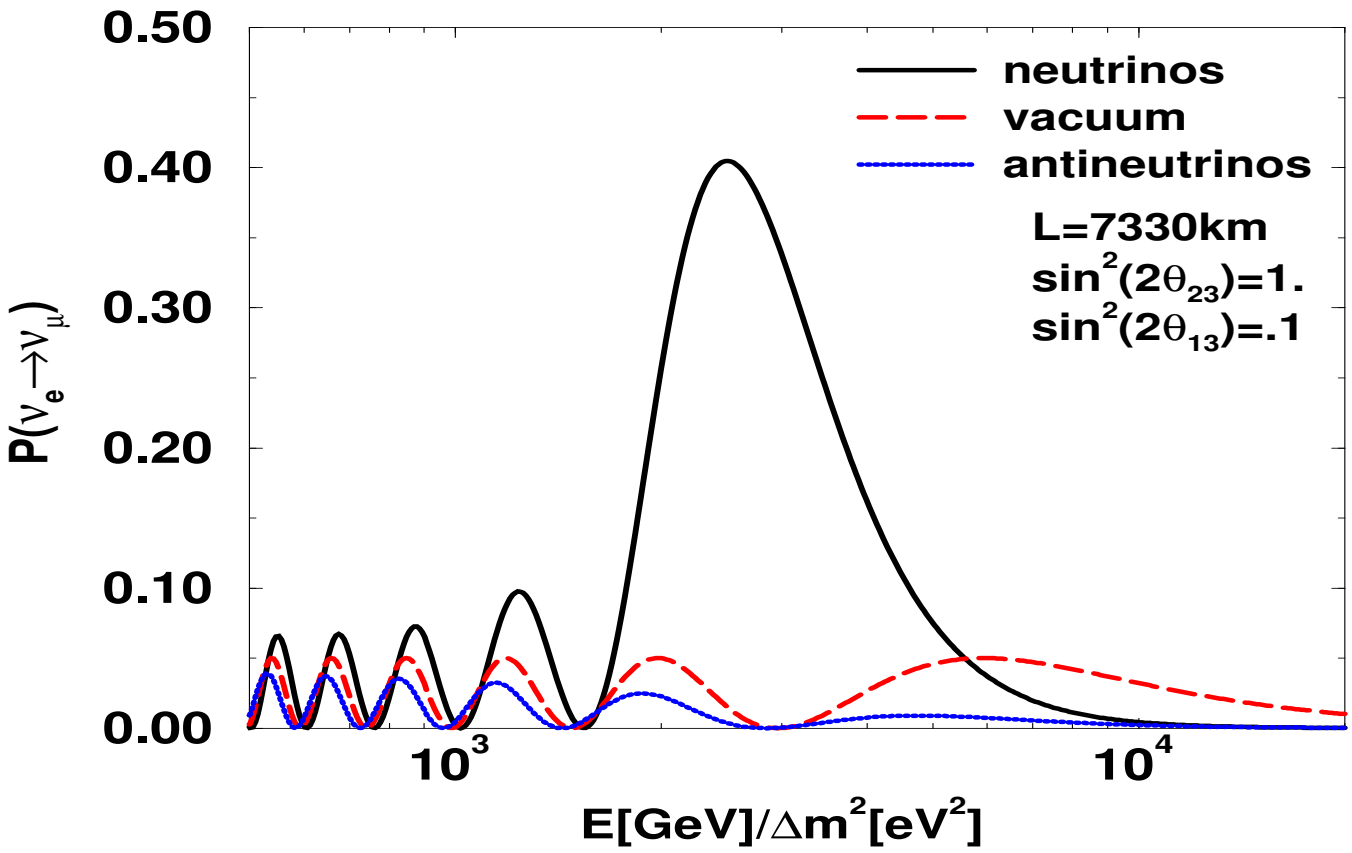
$E_\nu \gtrsim 2$ GeV, $\theta_n > 33.17^\circ$ (mantle crossing)

$$P_{3\nu}(\nu_\mu \to \nu_e) \cong \sin^2\theta_{23}\,\sin^2 2\theta^m_{13}\,\sin^2\frac{\Delta M^2_{31} L}{4E}$$

$\Delta m^2_{31} > 0$ **(NO):** $P_{3\nu}(\nu_{\mu(e)} \to \nu_{e(\mu)})$ **– resonantly enhanced,** $P_{3\nu}(\bar{\nu}_{\mu(e)} \to \bar{\nu}_{e(\mu)})$ **– suppressed.**

$\Delta m^2_{31} < 0$ **(IO):** $P_{3\nu}(\nu_{\mu(e)} \to \nu_{e(\mu)})$ **– suppressed,** $P_{3\nu}(\bar{\nu}_{\mu(e)} \to \bar{\nu}_{e(\mu)})$ **– resonantly enhanced.**

Earth matter effect in $\nu_\mu \to \nu_e$, $\bar{\nu}_\mu \to \bar{\nu}_e$ in the mantle (MSW)



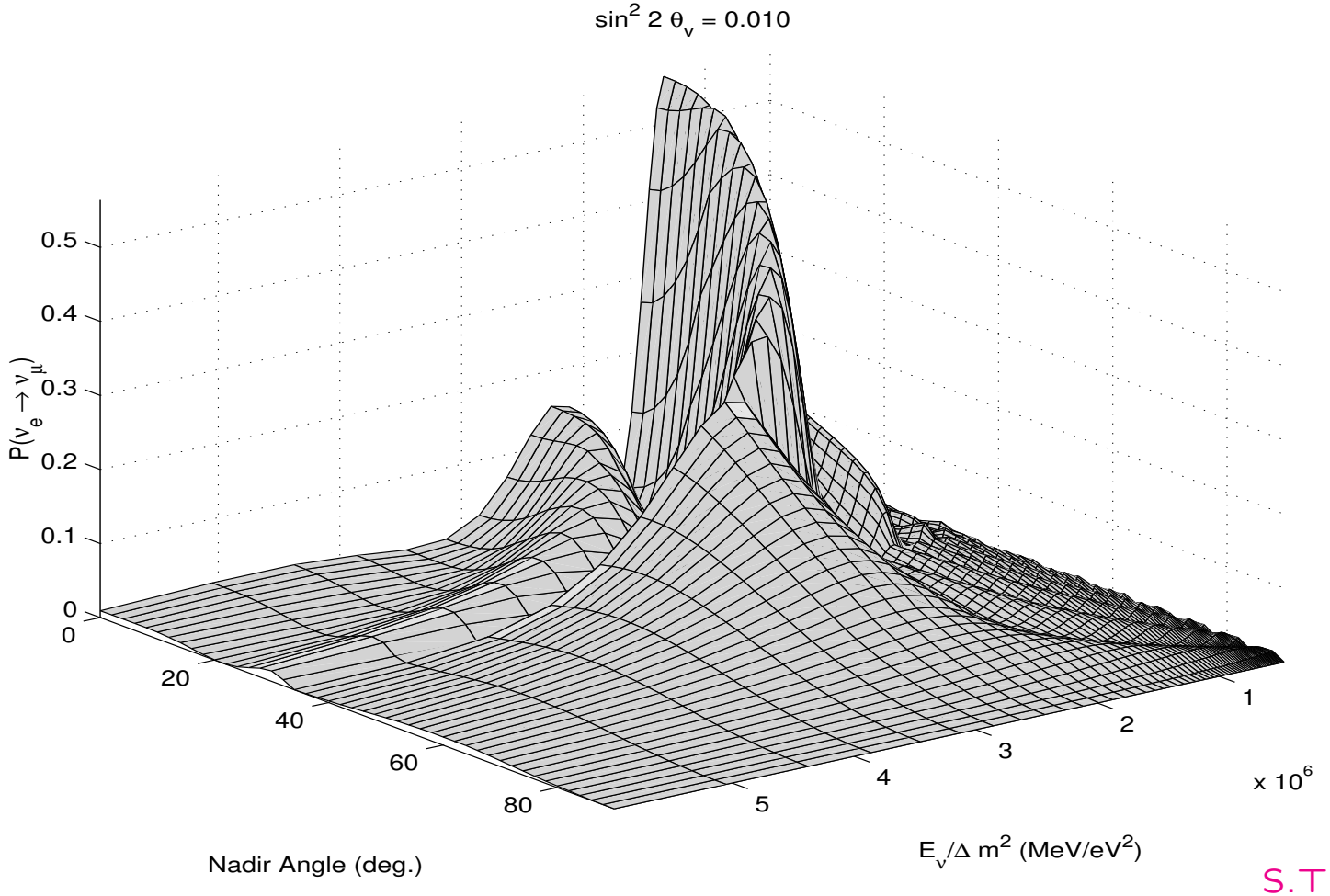
I. Mocioiu, R. Shrock, 2000

$\Delta m^2_{31} = 2.5 \times 10^{-3}$ eV^2, $E^{res} = 6.25$ GeV; $P^{3\nu} = \sin^2\theta_{23} P^{2\nu}_m = 0.5 P^{2\nu}_m$;
Maximum at $\rho^{res} = ((\Delta m^2_{31} \cos 2\theta_{13})/(2E\sqrt{2}G_F))(m_N/Y_e) = \bar{\rho}_{\rm man} \cong 4.6$ g/cm^{-3},
$L^{res}_m = L^v/\sin 2\theta_{13} \cong 6250/0.32$ km; $2\pi L/L_m \cong 0.75\pi (\neq \pi)$..

Sentivity to $\bar{\rho}_{\rm man}$ along the ν path in the mantle.

Resonance-like Amplification of Oscillations of Neutrinos Crossing the Earth Core

Earth matter effects in $\nu_\mu \to \nu_e$, $\bar{\nu}_\mu \to \bar{\nu}_e$ (NOLR)



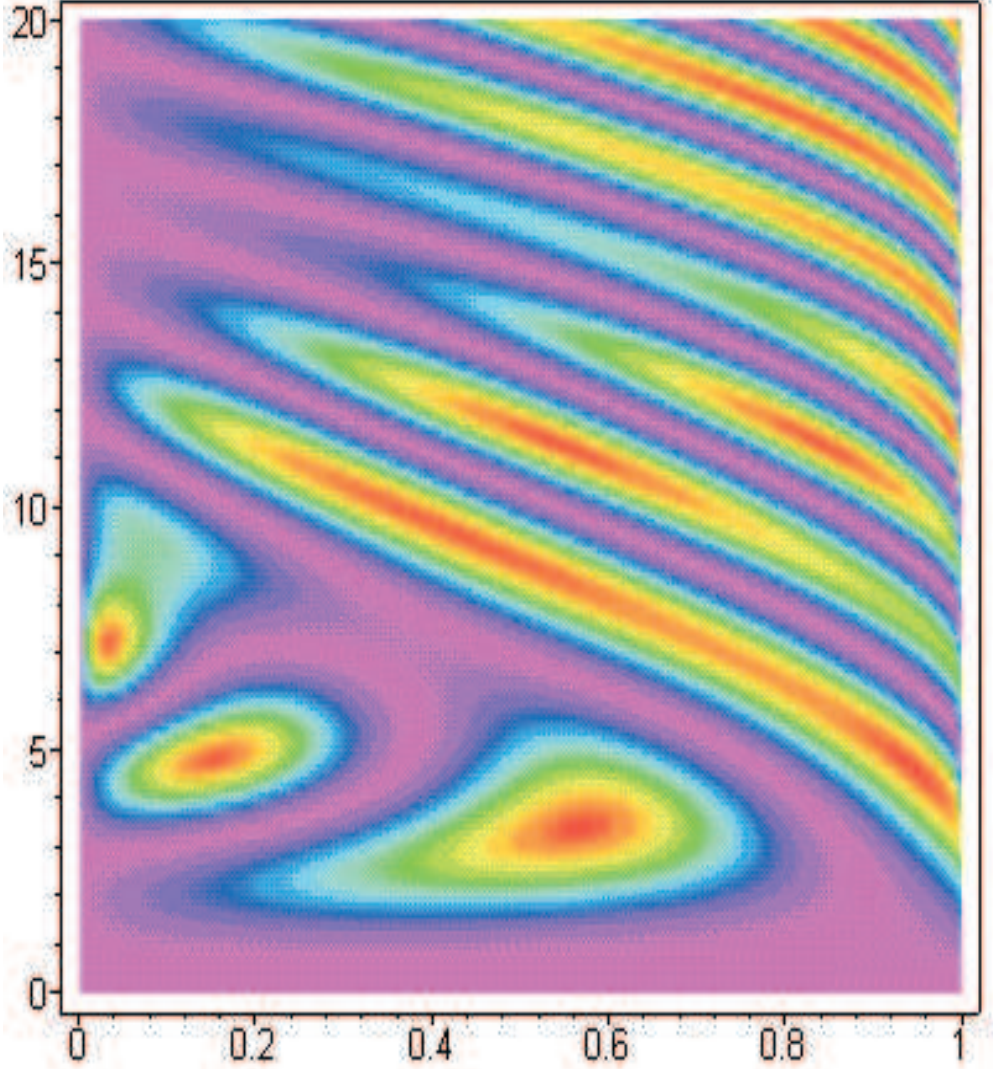
S.T.P., 1998; M. Chizhov, M. Maris, S.T.P., 1998; M. Chizhov, S.T.P., 1999

$P(\nu_e \to \nu_\mu) \equiv P_{2\nu} \equiv (s_{23})^{-2} P_{3\nu}(\nu_{e(\mu)} \to \nu_{\mu(e)})$, $\theta_v \equiv \theta_{13}$, $\Delta m^2 \equiv \Delta m^2_{31} > 0$;

Absolute maximum: Neutrino Oscillation Length Resonance (NOLR) :

$\rho_{man} < \rho^{res} < \rho_{core}$ **(NOLR≠MSW), sensitivity to** $\bar{\rho}_{\text{man}}$, $\bar{\rho}_{\text{core}}$.

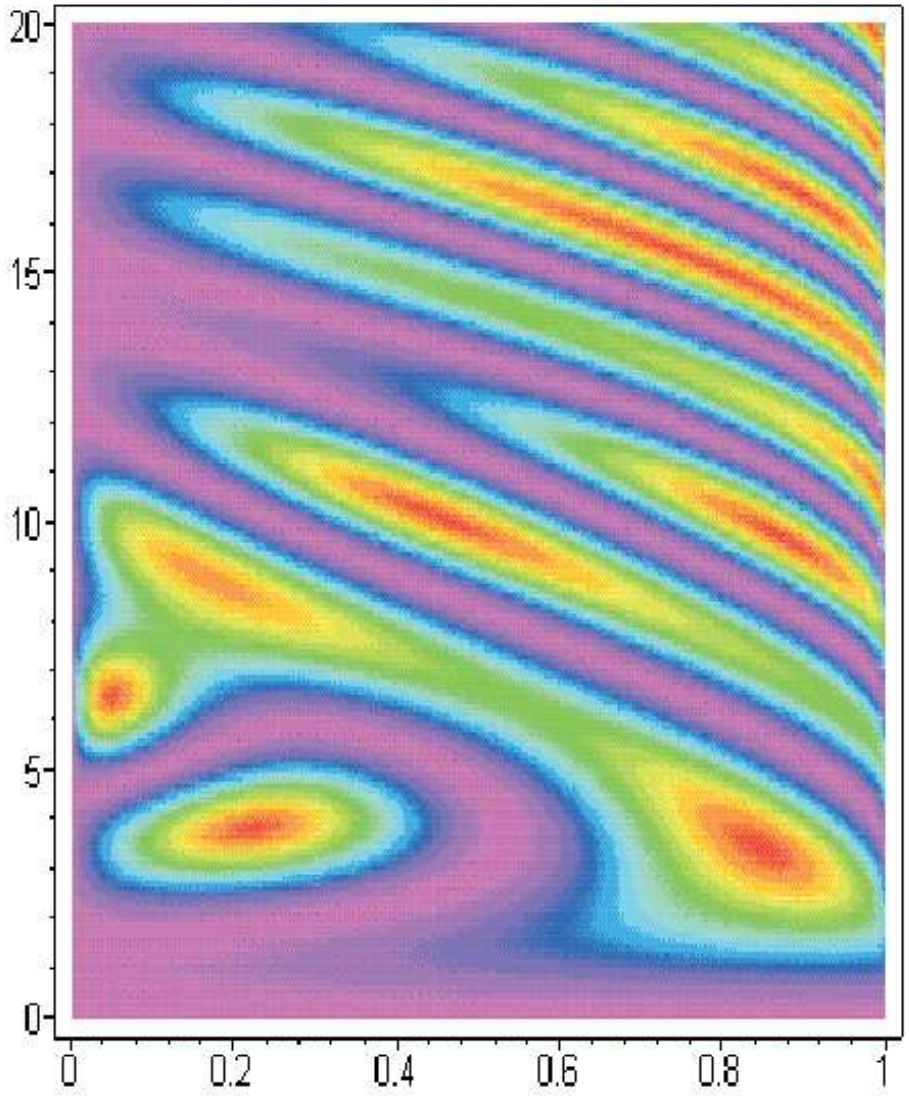
Local maxima: MSW effect in the Earth mantle or core.



$(s_{23})^{-2} P_{3\nu}(\nu_{e(\mu)} \to \nu_{\mu(e)}) \equiv P_{2\nu}$; **"Dark Red Spots"**, $P_{2\nu} = 0.9 - 1.0$;
NOLR: $P_{2\nu} = 1$ **at** $\sin^2 2\theta_{13} = 0.034;\ 0.154$, $E \cong 3.5;\ 5.2$ **GeV.**
Vertical axis: $\Delta m^2/E$ $[10^{-7} eV^2/MeV]$; **horizontal axis:** $\sin^2 2\theta_{13}$; $\theta_n = 0$

M. Chizhov, S.T.P., 1999 (hep-ph/9903399,9903424)

Sensitivity to $\bar{\rho}_{\text{man}}$, $\bar{\rho}_{\text{Core}}$, and to $(\bar{\rho}_{\text{Core}}/\bar{\rho}_{\text{man}})_{mcb}$ at mantle-core boundary.



The same for $\theta_n = 23^\circ$.
Vertical axis: $\Delta m^2/E$ $[10^{-7} eV^2/MeV]$; horizontal axis: $\sin^2 2\theta_{13}$.

M. Chizhov, S.T.P., 1999 (hep-ph/9903399,9903424)

• **For Earth center crossing ν's ($\theta_n = 0$) and, e.g. $\sin^2 2\theta_{13} = 0.01$, NOLR occurs at $E \cong 4$ GeV ($\Delta m^2(atm) = 2.5 \times 10^{-3}$ eV^2).**

S.T.P., hep-ph/9805262

• **For the Earth core crossing ν's: $P_{2\nu} = 1$ due to NOLR when**

$$\tan \Phi^{\text{man}}/2 \equiv \tan \phi' = \pm \sqrt{\frac{-\cos 2\theta''_m}{\cos(2\theta''_m - 4\theta'_m)}},$$

$$\tan \Phi^{\text{core}}/2 \equiv \tan \phi'' = \pm \frac{\cos 2\theta'_m}{\sqrt{-\cos(2\theta''_m)\cos(2\theta''_m - 4\theta'_m)}}$$

Φ^{man} (Φ^{core}) - **phase accumulated in the Earth mantle (core),**
θ'_m (θ''_m) - **the mixing angle (θ_{13}) in the Earth mantle (core).**

$P_{2\nu} = 1$ **due to NOLR for $\theta_n = 0$ (Earth center crossing ν's) at, e.g. $\sin^2 2\theta_{13} = 0.034;\ 0.154$, $E \cong 3.5;\ 5.2$ GeV ($\Delta m^2(atm) = 2.5 \times 10^{-3}$ eV^2).**

For E =3.5 GeV (5.2 Gev), the probability $P_{2\nu} \gtrsim 0.5$ for values of $\sin^2 2\theta_{13}$ from the interval $0.02 \lesssim \sin^2 2\theta_{13} \lesssim 0.10$ ($0.04 \lesssim \sin^2 2\theta_{13} \lesssim 0.26$).
The current b.f.v. of $\sin^2 2\theta_{13} = 0.084$.

M. Chizhov, S.T.P., Phys. Rev. Lett. 83 (1999) 1096 (hep-ph/9903399); Phys. Rev. Lett. 85 (2000) 3979 (hep-ph/0504247); Phys. Rev. D63 (2001) 073003 (hep-ph/9903424).

• **The first "oscillogram of the Earth" type figures appeared in M. Chizhov, M. Maris, S.T.P., hep-ph/9810501.**

The Earth matter effects in $\nu_{e(\mu)} \to \nu_{\mu(e)}$, $\bar{\nu}_{e(\mu)} \to \bar{\nu}_{\mu(e)}$, $\nu_e \to \nu_\tau$ and $\bar{\nu}_e \to \bar{\nu}_\tau$ oscillations are significant for $E_\nu \sim (2-10)$ GeV.

MSW in the Mantle: $E_\nu \sim (6-7)$ GeV ($|\Delta m^2_{31}| \equiv \Delta m^2(atm) = 2.5 \times 10^{-3}$ eV^2).

The mantle-core (NOLR) enhancement of $P^{2\nu}_m$ (or $\bar{P}^{2\nu}_m$):
$P_{2\nu} = 1$ due to NOLR for $\theta_n = 0$ (Earth center crossing ν's) at,
e.g. $\sin^2 2\theta_{13} = 0.034;\ 0.154$, $E \cong 3.5;\ 5.2$ GeV ($|\Delta m^2_{31}| = 2.5 \times 10^{-3}$ eV^2).

For E =3.5 GeV (5.2 Gev), the probability $P_{2\nu} \gtrsim 0.5$ for the values of $\sin^2 2\theta_{13}$ from the interval $0.02 \lesssim \sin^2 2\theta_{13} \lesssim 0.10$ ($0.04 \lesssim \sin^2 2\theta_{13} \lesssim 0.26$).
The current b.f.v. of $\sin^2 2\theta_{13} = 0.084$.

The effects of Earth matter on the oscillations of atmospheric (and accelerator) neutrinos have not been observed so far; can be used for performing tomography of the Earth with neutrinos having $E_\nu \sim (2-10)$ GeV (DUNE: $E_\nu \sim 0.2$ GeV, K.J. Kelly et al., arXiv:2110.00003, requires detection of protons in $\nu_{\mu(e)} + n \to \mu^-(e^-) + p$).

The fluxes of atmospheric $\nu_{e,\mu}$ of energy E, which reach the detector after crossing the Earth along a given trajectory specified by the value of θ_n, $\Phi_{\nu_{e,\mu}}(E,\theta_n)$, are given by the following expressions in the case of the 3-neutrino oscillations under discussion and $E_\nu \gtrsim 2$ GeV:

$$\Phi_{\nu_e}(E,\theta_n) \cong \Phi^0_{\nu_e}\left(1 + [s^2_{23} r - 1]\ P^{2\nu}_m\right),$$

$$\Phi_{\nu_\mu}(E,\theta_n) \cong \Phi^0_{\nu_\mu}\left(1 + s^4_{23}[(s^2_{23}\ r)^{-1} - 1]P^{2\nu}_m - 2c^2_{23}s^2_{23}\left[1 - Re\ (e^{-i\kappa}A^{2\nu}_m(\nu_\tau \to \nu_\tau))\right]\right),$$

where $\Phi^0_{\nu_{e(\mu)}} = \Phi^0_{\nu_{e(\mu)}}(E,\theta_n)$ is the $\nu_{e(\mu)}$ flux in the absence of neutrino oscillations and

$$r \equiv r(E,\theta_n) \equiv \frac{\Phi^0_{\nu_\mu}(E,\theta_n)}{\Phi^0_{\nu_e}(E,\theta_n)} \quad .$$

$r = 2$, $s^2_{23} = 0.5$: $[s^2_{23} r - 1] = 0$

s^2_{23}: b.f.v. 0.470 (0.550) NO (IO); 3σ CL: (0.435 (0.440)-0.585 (0.584) .

F. Capozzi et al., 2107.00532; M.C. Gonzalez-Garcia et al., 2111.03086

$r(E,\theta_n) \cong (2.6 \div 4.5)$ for neutrinos giving the main contribution to the multi-GeV samples, $E \cong (2 \div 10)$ GeV.

M. Honda, 1995.

$E_\nu \sim 0.2$ GeV, r = 2 (DUNE):

$$\Phi_{\nu_e}(E,\theta_n) \cong \Phi^0_{\nu_e}\left(1 + [c^2_{23} r - 1]\ P^{2\nu}_m\right) \cong \Phi^0_{\nu_e}, \text{ if } c^2_{23} = 0.5\,.$$

The Earth matter effects in the $\nu_{\mu(e)} \to \nu_{e(\mu)}$ ($\bar{\nu}_{\mu(e)} \to \bar{\nu}_{e(\mu)}$) oscillations depend on

$$V =^{+}_{(-)} \sqrt{2}\, G_{\mathsf{F}}\, N_e^{(E)}(r)$$

$$N_e^{(E)}(r) = \rho_{\mathsf{E}}(r)\, Y_e/m_{\mathsf{N}},$$

Y_e **- electron fraction number (or Z/A factor).**

For isotopically symmetric matter $Y_e = 0.5$.

Earth core composition models: $Y_e^c = 0.466 - 0.471$.

Earth mantle composition models: $Y_e^{man} = 0.490 - 0.497$.

Varying Y_e^c and Y_e^{man} in the indicated respective intervals has no effect on the results on the $\bar{\rho}_{\mathsf{man}}$, $\bar{\rho}_{\mathsf{C}}$ $\bar{\rho}_{\mathsf{OC}}$, $\bar{\rho}_{\mathsf{IC}}$ determination using the neutrino oscillation tomography method.

Determining the composition of, e.g., the OC or IC is technically a very different problem with respect to determining $\bar{\rho}_{\mathsf{man}}$, $\bar{\rho}_{\mathsf{C}}$ $\bar{\rho}_{\mathsf{OC}}$, $\bar{\rho}_{\mathsf{IC}}$: does not require varying $\bar{\rho}_{\mathsf{i}}$ in the study.

Important Constraints

The total Earth mass constraint:

$$M_\oplus = (5.9722 \pm 0.0006) \times 10^{24} \text{ kg}$$

Earth momentum of inertia constraint:

$$I_\oplus = (8.01736 \pm 0.00097) \times 10^{37} \text{ kg m}^2.$$

$$I_\oplus = 0.330745\, M_\oplus\, R_\oplus^2.$$

Earth hydrostatic equilibrium (EHSE) constraint:

$\rho_{man} < \rho_{OC} < \rho_{IC}$, **or, for example,**

$$\rho_{uman} < \rho_{lman} < \rho_{OC} < \rho_{IC}$$

Neutrino Oscillation Tomography of the Earth with the Hyper-Kaiokande Detector

C. Jesús-Valls, S.T.P., J. Xia, EPJ C85 (2025) 703 [arXiv:2411.12344]

Disclaimer: this study is not a study by the Hyper-Kamiokande collaboration.

Aspects of the Analysis

We change the PREM density in a given layer $\rho_i(r)$, $i = \mathrm{IC}, \mathrm{OC}, \mathrm{man}$, by a factor $(1 + \kappa_i)$, κ_i is r-independent real constant:

$$\rho_i(r) \to \rho_i'(r) = (1 + \kappa_i)\rho_i(r).$$

We will present results on sensitivity of HK to

$$\Delta\rho_i = 100\%\,((1 + \kappa_i)\rho_i(r) - \rho_i(r))/\rho_i(r) = 100\%\,\kappa_i.$$

When we increase (decrease) the density in one layer, in order to keep $M_\oplus$ and $I_\oplus$ unchanged, we have to decrease (increase) the density in at least two other layers. The factor by which that has to be done depends on the relative volumes and densities of the layers. In our study we have accounted for both the $M_\oplus$ and $I_\oplus$ constraints when varying $\rho_i(r)$.

To be more specific, in the standard 3-layer model of the Earth, consisiting of mantle, outer core and inner core, when we consider, e.g., variation of $\bar{\rho}_{\rm OC}$, we compensate it by the corresponding change of density of the inner core $\bar{\rho}_{\rm IC}$ and of the mantle $\bar{\rho}_{\rm man}$.

Using the PREM averagde densities we have:

$$M_\oplus = M_\oplus(\bar{\rho}'_{\rm IC}, \bar{\rho}'_{\rm OC}, \bar{\rho}'_{\rm man}) = M_\oplus(\kappa_{\rm IC}, \kappa_{\rm OC}, \kappa_{\rm man}),$$
$$I_\oplus = I_\oplus(\bar{\rho}'_{\rm IC}, \bar{\rho}'_{\rm OC}, \bar{\rho}'_{\rm man}) = I_\oplus(\kappa_{\rm IC}, \kappa_{\rm OC}, \kappa_{\rm man}) \ ,$$

i.e., two equations for three unknowns. We can express, e.g., $\kappa_{\rm IC}$ and $\kappa_{\rm man}$ in terms of $\kappa_{\rm OC}$.
By using the EHE constraint $\bar{\rho}'_{\rm man} < \bar{\rho}'_{\rm OC} < \bar{\rho}'_{\rm IC}$ we can obtain the ranges of variation of $\kappa_{\rm OC}$, and consequently of $\kappa_{\rm IC}$ and $\kappa_{\rm man}$ that are allowed by the $M_\oplus$, $I_\oplus$ and EHE constraints.

Numerically we find (the lower bound on κ_{OC}, $\kappa_{IC} \leq 0.25(0.50)$):

$$-0.018\ (0.036) \lesssim \kappa_{OC} < 0.010\,.$$

$$-1.15 \times 10^{-3} \lesssim \kappa_{man} < 0.060\,.$$

$$-0.145 \lesssim \kappa_{IC} < 7.62\,;\ use\ < 0.25\ (0.50).$$

S.T.P., 2406.13727

These very restrictive constraints can be traced to the relatively small contributions of the inner core to $M_\oplus$ and especially to $I_\oplus$. The observation of such small variations of κ_{OC} and is beyond the reach of all currently running, under construction and planned experiments.

Therefore we have considered the case of two different mantle layers and the core layer. The mantle is divided into
i) lower mantle, extending from $R_c = 3480$ km to $R_{\rm lman} = 5701$ km, with PREM density $\bar{\rho}_{\rm lman} = 4.9035$ g/cm^3, and
ii) upper mantle, extending from $R_{\rm lman} = 5701$ km to $R_{\rm man} = 6346.6$ km, with PREM density $\bar{\rho}_{\rm uman} = 3.6046$ g/cm^3.
One finds that in this case the $M_\oplus$, $I_\oplus$ and the EHE constraint in the form $\bar{\rho}'_{\rm uman} < \bar{\rho}'_{\rm lman} < \bar{\rho}'_{\rm C}$ lead to:

- $0.33 < \kappa_{\rm C} < 0.09\,, \quad 7.36 < \bar{\rho}'_{\rm C} < 11.98$ g/cm^3,
- $0.13 < \kappa_{\rm lman} < 0.48\,, \quad 4.26 < \bar{\rho}'_{\rm lman} < 7.25$ g/cm^3,
- $0.69 < \kappa_{\rm uman} < 0.18\,, \quad 1.12 < \bar{\rho}'_{\rm uman} < 4.23$ g/cm^3.

S.T.P., 2406.13727; C. Jesus-Valls, S.T.P., J.Xia, 2411.12344

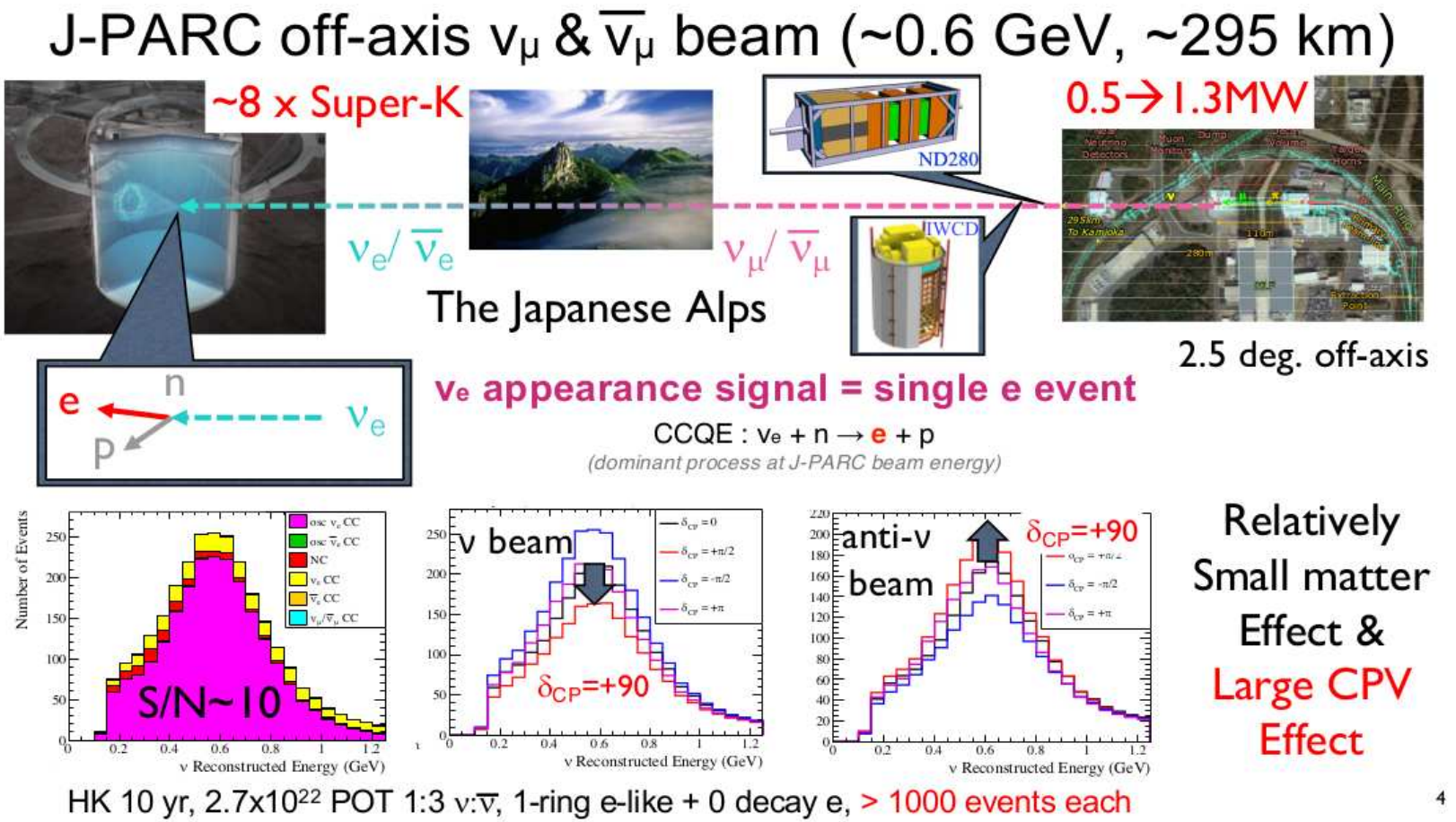
We have implemented these constraints in our analysis.

Hyper-Kamiokande and T2HK

Hyper-Kamiokande: water-Cherenkov, ~ 025 Mton, fiducial ~ 0.2 Mton; 2028; T2HK.



The next slides are from the talk by S. Muriyama at Neutrino 2024.

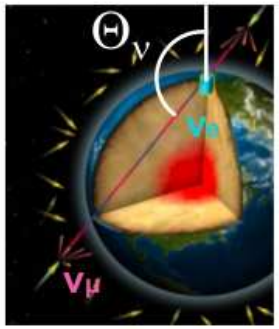


Atmospheric 3-flavor ν beam (0.1-10^3 GeV, 10-13,000 km)

- The wide range of E (0.1~10^3 GeV) and L (10 km ⬇ ~13,000 km ⬆) provide an excellent opportunity to study various properties of ν.
- Study of the earth matter effect to determine neutrino mass ordering
- Unique tests of exotic properties

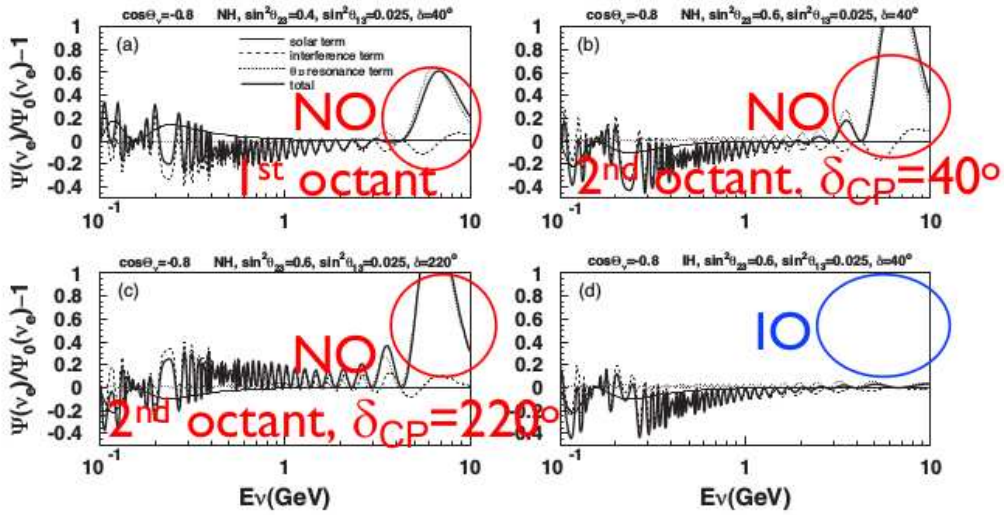
~80 events/day

Oscillation studies with wide range of E and L. The matter effect solves MO.



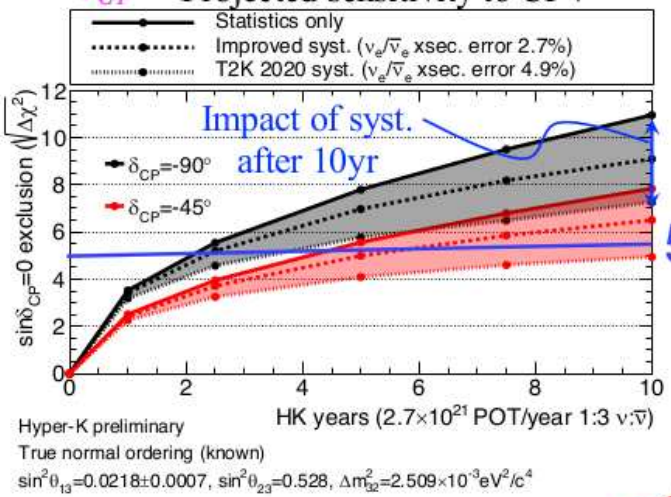
In case of $\cos\Theta_\nu$=-0.8, the effect of MO can be observed.

Effect of Mass Ordering (MO) and $\not{CP}$ on ν_e flux

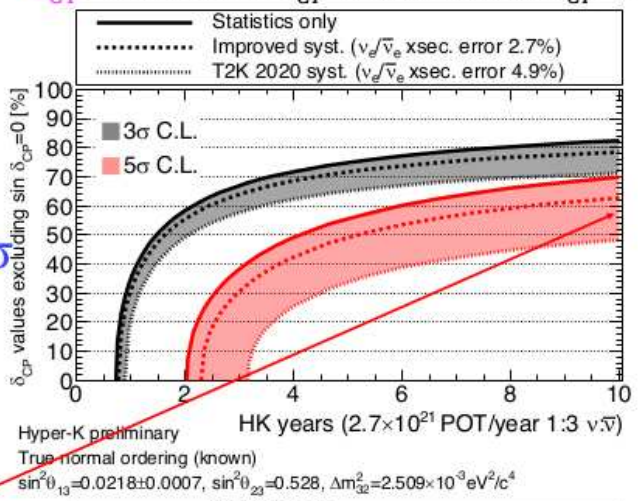


Precision measurement of neutrino oscillations

δ_{CP} Projected sensitivity to CPV



δ_{CP} Fraction of δ_{CP} to exclude $\sin\delta_{CP} = 0$



5σ

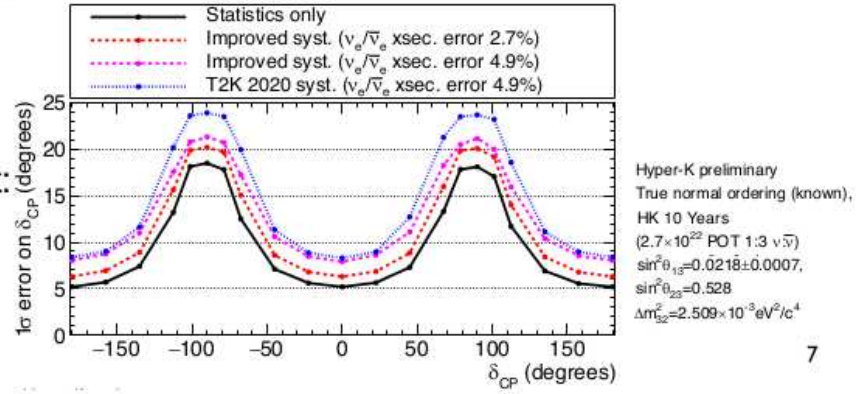
Discovery of CP violation at >5 σ for >60% of δ_{CP}

1σ resolution of δ_{CP} in 10 yrs

~20° for $\delta_{cp} = -90°$ / ~6° for $\delta_{cp} = 0°$

Reduction of systematic uncertainty has sizable impact:

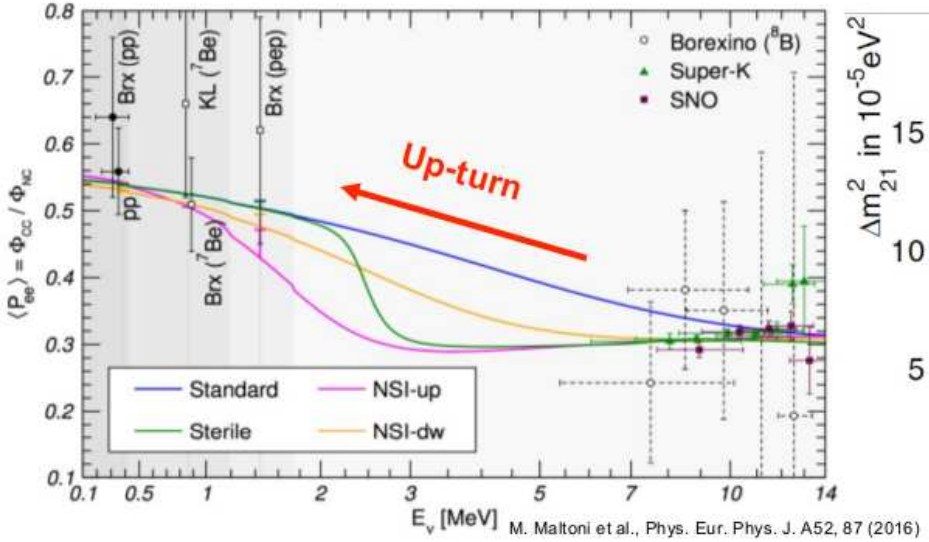
- Upgrade of ND280 + ~600 ton Intermediate Water Cherenkov detector (IWCD)
- Aim to suppress detector error below 1%

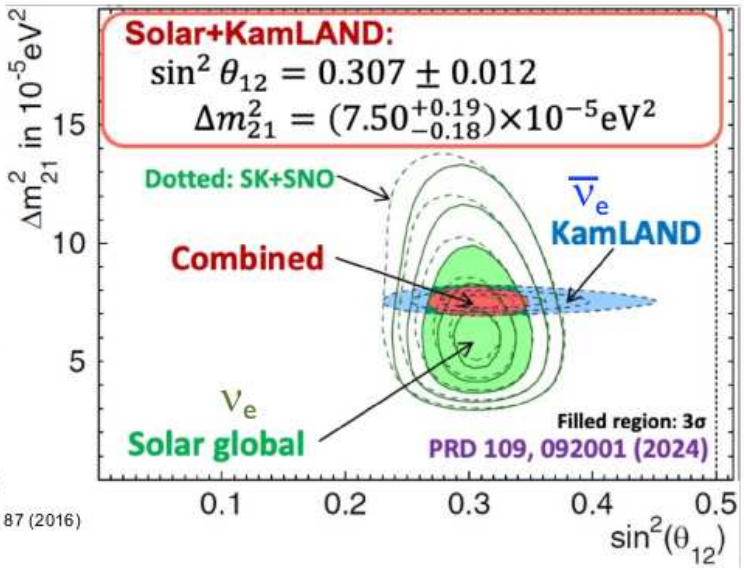


Solar ν spectrum & possible differences in $\nu_e/\overline{\nu}_e$ oscillation

Confirm MSW effect by observing spectrum distortion "up-turn"

Compare ν_e, $\overline{\nu}_e$ oscillation (currently ~1.5σ tension in solar/reactor ν)



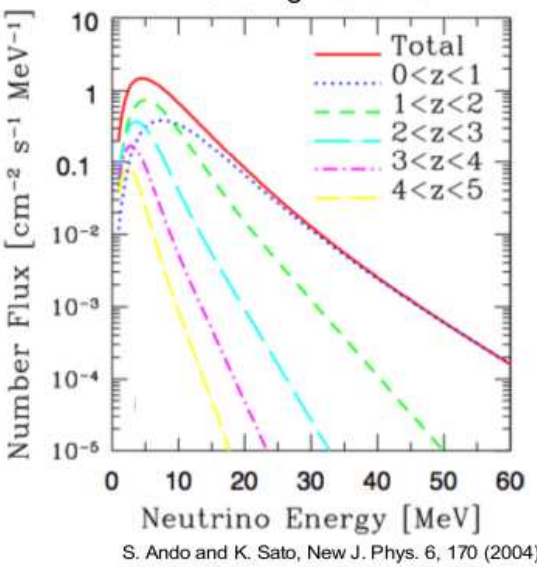


~130 events/day

- > 3σ sensitivity for the spectrum up-turn in 10 yrs (E_{th}=4.5 MeV).
- ~2σ day/night sensitivity expected for the difference in $\nu_e/\overline{\nu}_e$ osc. in 20 yrs.

Diffuse Supernova Neutrino Background (DSNB)

DSNB energy spectrum including red shift

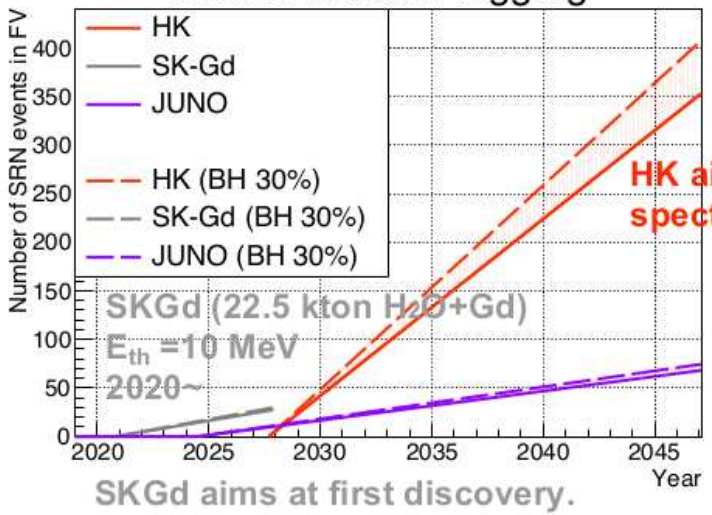


S. Ando and K. Sato, New J. Phys. 6, 170 (2004)

$$\frac{dF_\nu}{dE_\nu} = \frac{c}{H_0}\int_0^{z_{max}} R_{SN}(z)\frac{dN_\nu(E'_\nu)}{dE'_\nu}\frac{dz}{\sqrt{\Omega_m(1+z)^3+\Omega_\Lambda}},$$

Neutrinos from supernova explosions in the early universe to the present day integrated flux ~10 $cm^{-2}sec^{-1}$

Number of DSNB events before neutron tagging



SKGd aims at first discovery.

HK (187 kton H_2O)
E_{th} =16 MeV
2027~

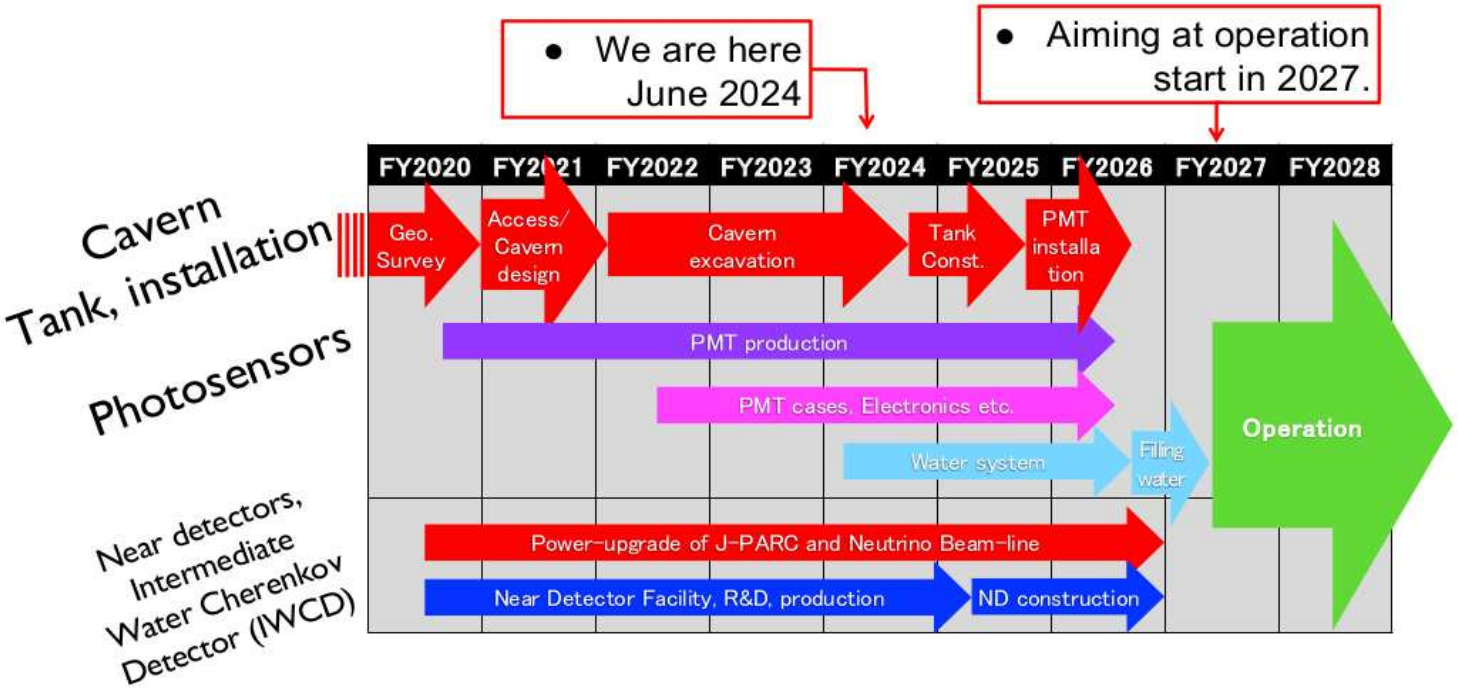
HK aims for precise flux & spectrum measurement.

JUNO (20 kt LS)
E_{th} =12 MeV
2024~

~4 ev/yr after neutron tagging w/ H_2O

- Stellar collapse
- Star formation rate
- Heavy element synthesis

Construction Schedule



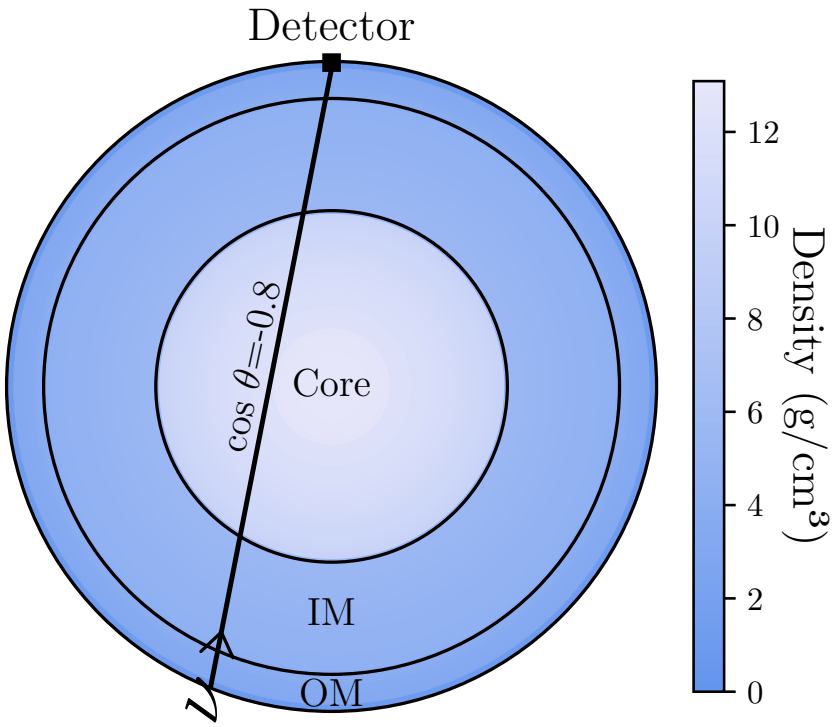
Summary

- Hyper-K will play a central role in exploring the future of particle physics and contribute to the future of astronomy. Expectations in 10 yrs HK:
  - Mass ordering: 3.8-6.2σ depending on $\sin^2\theta_{23}$
  - CP violation: 5σ discovery, > 60%
  - Proton decay: $p \rightarrow e^+\pi^0$: ~6×10^{34} yrs etc.
  - > 3σ sensitivity for the solar ν spectrum up-turn
  - ~70k events @10 kpc supernova
  - ~4 events/yr diffuse supernova neutrino background
- The highlight of the civil construction, the dome excavation, was completed. Detailed design of tank lining and photosensor support structure completed.
- 50 cm PMT delivery is ongoing and on schedule.
- Beam intensity increase/IWCD construction is on the way.
- Data-taking is expected to start in 2027!

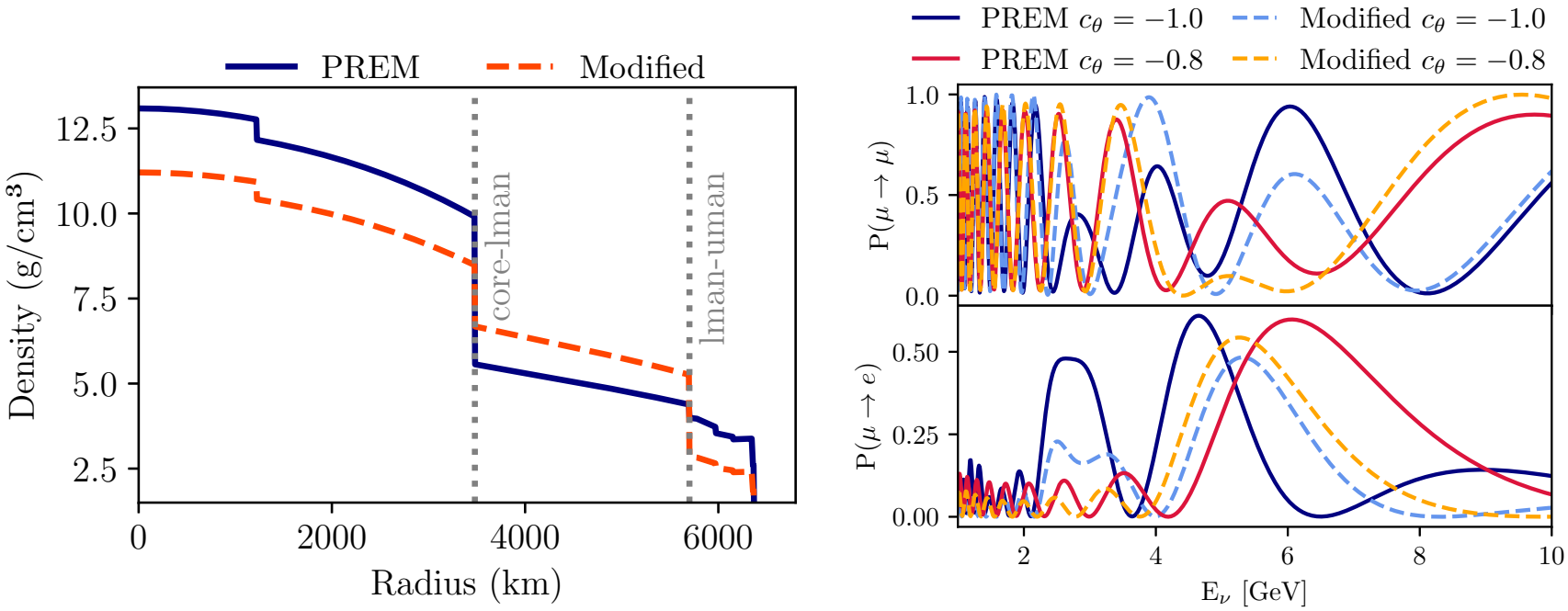
23

Scheduled to star data-taking on April 1, 2028.

Aspects of the Analysis



A diagram of the Earth interior under study. The angle $\cos\theta = -1$ corresponds to an up-going neutrino crossing the Earth along the diameter before being detected.



Left panel: Earth density according to PREM and an example solution for a modified Earth with fixed $\kappa_{lman} = 0.2$.
Right panel: ν_ν disappearance and ν_e appearance probabilities for two values of the azimuth angle and the Earth models shown in the left panel.

Analysis Methodology

This study uses the public release (Zenodo, Oct. 4, 2023. doi: 10.5281/zenodo.8401262) simulated atmospheric neutrino event rate predictions generated by the Super-Kamiokande (SK) collaboration in its latest atmospheric neutrino oscillation analysis (Phys. Rev. D 109 (2024) 072014 [arXiv:2311.05105]). It consists of the expected event rates, and one-dimensional true energy and angle event distributions for a list of 931 angle and energy bins divided in 29 samples, corresponding to 29 different sets of event selection conditions. The distributions are released as 1D true neutrino energy and true azimuth angle quantiles at 2.3%, 15.9%, 50%, 84.1% and 97.7% of the distribution. The predictions are divided in three major blocks, consisting of the unoscillated, and oscillated predictions assuming either the normal or the inverted mass ordering. For each, the predictions are divided in six components: ν_e, ν_μ, $\bar{\nu}_e$, $\bar{\nu}_\mu$, $\nu_\tau + \bar{\nu}_\tau$ and neutral current (NC). Additionally, the measured data counts in every bin are provided.

The 29 selections samples can be sub-divided in 19 samples without and 10 with neutron tagging, often indicated with additional labels `0 n`, `1 n`, etc. This large number of samples is the result, in part, to splitting some samples in two phases of the Super-Kamiokande experiment, i.e. data from SK runs 1 to 3 and from runs 4 to 5, further details on the specifics of this data periods are availabel in Phys. Rev. D 109 (2024) 072014 [arXiv:2311.05105].

Broadly speaking there are 4 different categories of samples: Sub-GeV

samples, Multi- GeV samples, NC-samples, and non-fully-contained (non-FC) samples. Oscillations of neutrinos with energy below 1 GeV change very rapidly with energy and azimuth angle, see previous Fig. 2, such that tomography-sensitive variations get largely averaged out. Therefore we do not consider Sub-GeV samples. Similarly, as our interest regards effects in the neutrino flux flavor composition, we do not include NC-samples, insensitive to flavor transitions. Lastly, we only consider those samples that have a significant fraction of events with energies of interest. Accordingly, we ignore the Up-μ showering and Up-μ stopping samples, which largely consist of events with energies above several tens of GeV.

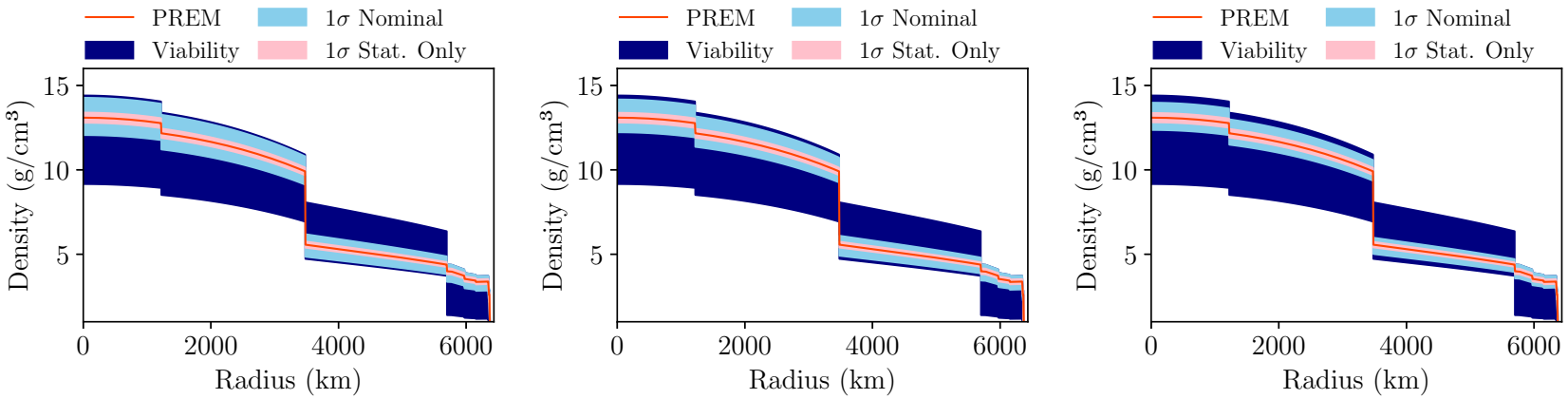
Therefore, in this analysis we utilize a total of 12 selection samples, consisting of Multi-GeV events with a single lepton ring (ν_μ, $\bar{\nu}_\mu$, ν_e, $\bar{\nu}_e$ 0 n, $\bar{\nu}_e$ 1 n) and Multi-GeV events with multiple rings (ν_μ, ν_e, $\bar{\nu}_e$ and other), and non-FC events (partially contained stopping, partially contained through-going and Up-μ stopping).

Our analysis includes realistic flux (M. Honda et al., Phys. Rev. D83 (2011) 123001 [arXiv:1102.2688]), neutrino interaction modeling using NEUT (Y. Hayato, L. Pickering, EPJ ST 230 (2021) 4469), detector effects and analysis sample selection criteria. Based on those simulations, we extrapolate the Earth tomography sensitivity to Hyper-Kamiokande (HK), a detector eight times larger than SK, but based on the same detection concept and with small instrumentation differences. Additionally, we modify the nominal distributions to assess the potential impact of enhanced energy and/or angular resolutions in HK.

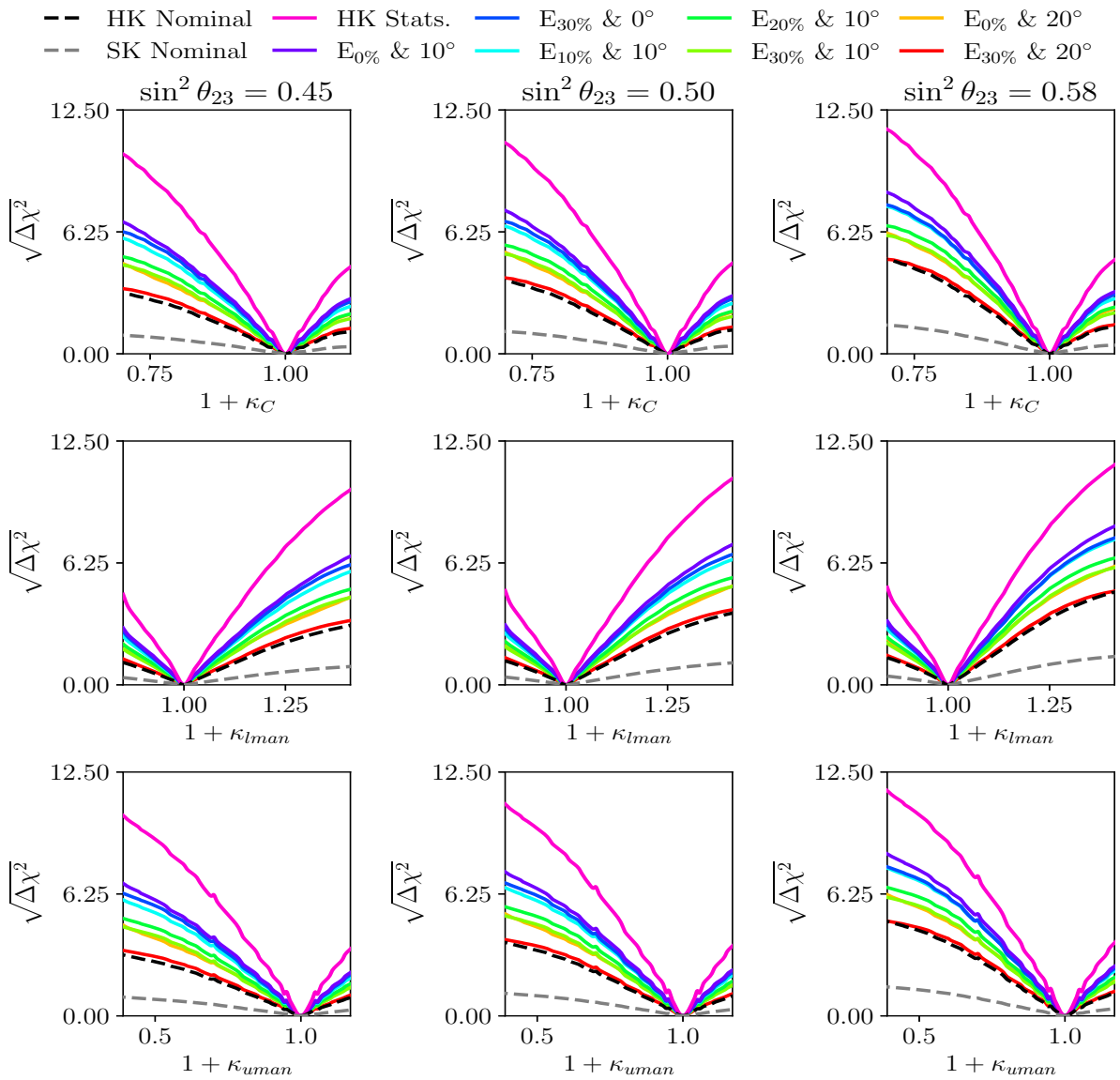
Oscillation probability evaluation

The 3-flavour oscillation probability is evaluated using the `Prob3++` framework (for detaila see https://github.com/rogerwendell/Prob3plusplus), developed by Super-Kamiokande collaborators. The framework calculates the oscillation probability including matter effects for any neutrino flavor transition as a function of the input PMNS parameters, the values of the neutrino mass squared differences values, and the Earth model configuration, which is input as a collection of density values along the Earth radius. `Prob3++` takes as input the Earth density profile given by a collection of points. We evaluate the Earth density at 82 points along the Earth radius. A subset of 61 points are distributed from 0 to 5600 km every 100 km, with few additional points near the shell transitions. The remaining points describe the 5600 km to 6371 km region, sampled more frequently at irregular intervals to reflect the finer structure of the Earth crust.

Results



Confidence intervals of HK sensitivity to deviations of the core, lower mantle and upper mantle average densities from their respective PREM values. The dark blue bands correspond to varying κ_C in the interval $-0.30 < \kappa_C < 0.10$, allowed by the Earth total mass, moment of inertia and hydrostatic equilibrium constraints. The light blue and red bands represent the 1σ *Nominal* ($E_{30\%}$ & 20°) and *Stats.Only* (E_0 & 0°) confidence level intervals. The left, center and right panels correspond respectively to $\sin^2\theta_{23} = 0.45$, 0.50, 0.58.



Sensitivity to deviations of the Earth core, lower mantle and upper mantle densities from their respective PREM values, parametrised as $\rho_i(1+\kappa_i)$, $i = c, lman, uman$, ρ_i being the PREM densities, for different HK detector configurations. The left, center and right columns correspond to: $\sin^2\theta_{23} = 0.45$, 0.50 and 0.58.

We find, in particular, that for $\sin^2\theta_{23} = 0.5$ and the "nominal" energy and zenith angle resolutions of $E_{30\%}$ & 20° in all samples, after 6500 days of operation the HK experiment can determine the Earth core average density at 2σ C.L. with a relative uncertainty $\Delta\bar{\rho}_C/\bar{\rho}_C = 100\%\kappa_C$ of (-14.5%)/+39.5 ($-0.145 \leq \kappa_c \leq 0.395$).
For $\sin^2\theta_{23} = 0.58$ the uncertainty is noticeably smaller: (-9.3%)/+31.7% ($-0.093 \leq \kappa_c \leq 0.317$).
The sensitivity of the HK experiment will be much higher in the case of energy and angular resolutions of $E_{20\%}$ & 10°. It increases also significantly with $\sin^2\theta_{23}$. Indeed, in this case at 2σ C.L. we have for $\sin^2\theta_{23} = 0.45$, 0.50 and 0.58, respectively: (-9.2%)/+11.3% ($-0.092 \leq \kappa_c \leq 0.113$), (-8.3%)/+9.8% ($-0.083 \leq \kappa_c \leq 0.098$) and (-6.7%)/+8.5% ($-0.067 \leq \kappa_c \leq 0.085$) .
Thus, if, e.g., $\sin^2\theta_{23} = 0.50$, the HK experiment would be able to establish that the average core density at 2σ C.L. lies in the rather narrow interval: $10.08\ \text{g/cm}^3 \leq \bar{\rho}_C \leq 12.06$ g/cm^3, with the PREM value of $\bar{\rho}_C = 10.99$ g/cm^3.

Similarly, it will follow from the HK data that at 2σ C.L. the average lower and upper mantle densities, have values in the intervals: $4.49\ \text{g/cm}^3 \leq \bar{\rho}_{lman} \leq 5.38\ \text{g/cm}^3$, $3.00\ \text{g/cm}^3 \leq \bar{\rho}_{uman} \leq 4.25\ \text{g/cm}^3$. We recall that the PREM values of $\bar{\rho}_{lman}$ and $\bar{\rho}_{uman}$ are $4.90\ \text{g/cm}^3$ and $3.60\ \text{g/cm}^3$, respectively.

Given the PREM values of $\bar{\rho}_{man} = 4.66$ g/cm^3 and $\bar{\rho}_{IC} = 12.89$ g/cm^3, the HK result on $\bar{\rho}_C$ would be an independent confirmation of the existence of at least three major density layers in the interior of the Earth.

Our results show that the Hyper-Kamiokande experiment, after collecting a sufficiently large data sample, can make a major contribution to the tomography studies of the Earth interior with neutrinos.

General Observations

The neutrino tomography of the Earth – two different sets of goals:
A. information about the densities of the different Earth layers,
B. information about the composition of the different layers.

The set A. includes.

– Getting information about the mantle (upper, lower), core, outer core, inner core densities.

– Getting information about the location and the width of, and the changed of density in, the manlte-core transtions zone.

– Getting information about the OC - IC transition (location, width of the zone, jump of density).

The set B. includes.

Getting information about the compositions of the OC, IC and other possible layers (e.g., lower mantle, the composition of the mantle-core transition zone).

The sensitivity is maximal for the largest allowed value of $\sin^2\theta_{23}$ **and for NO in the case of the effects in the interval** $E_\nu \sim (2-10)$ **GeV (or** $E_\nu \sim (100-300)$ **MeV).**

Some of the goals (especially those related to the inner core and the composition of the various layers) are extremely challenging but worth the efforts.

From the studies performed so far it follows that using the neutrino oscillation tomography method it is very difficult to get information about $\rho_{\rm IC}(r)$ and the IC-OC transition zone.

Thus, getting information about $\rho_{\rm IC}(r)$ and about the the OC-IC transition ($\rho_{\rm IC}(r)/\rho_{\rm OC}(r)$ at the transition) – remarkably challenging problem.

Determine the experimental conditions (statistics, systematics, resolutions, efficiencies of identification of the different types of events, etc.) that could allow to achieve each of the different goals.
Should be done for each of the detectors that can be used for neutrino tomography of the Earth.

In setting the specific goals the collaboration with the colleagues-geophysicists is extremely importatnt.

Important Constraints

The total Earth mass constraint:

$$M_\oplus = (5.9722 \pm 0.0006) \times 10^{24} \text{ kg}$$

Earth hydrostatic equilibrium constraint:

$$\rho_{man} \leq \rho_{OC} \leq \rho_{IC}.$$

Earth momentum of inertia constraint:

$$I_\oplus = (8.01736 \pm 0.00097) \times 10^{37} \text{ kg m}^2.$$

$$I_\oplus = 0.330745\, M_\oplus\, R_\oplus^2.$$

The three constraints should always be implemented in the simulations.

Typically in the analyses of the sensitivity of a given experiment to the density in a given Earth layer, one changes the PREM density in a given layer $\rho_i(r)$, $i = \mathrm{IC}, \mathrm{OC}, \mathrm{man}$, by a factor $(1 + \kappa_i)$, κ_i is r-independent real constant:

$$\rho_i(r) \to (1 + \kappa_i)\rho_i(r).$$

In order to satisfy the $M_\oplus$ and $I_\oplus$ constraints, one has to correspondingly change the density in two other Earth layers.

The sensitivity to a given $\rho_i(r)$ depends strongly on, e.g., whether the $M_\oplus$ ($M_\oplus$ and $I_\oplus$) and EHE constraints are implemented or not, and – if they are implemented– on how they are implemented.

The results are very different if the $M_\oplus$ ($M_\oplus$ and $I_\oplus$) EHE constraints are not implemented.

In the PREM model, widely used in neutrino tomography of the Earth studies, $\rho_{\rm E}$ is assumed to be spherically symmetric, $\rho_{\rm E} = \rho_{\rm E}(r)$, r being the distance from the Earth center, and there are two major density structures - the core and the mantle, and a certain number of substructures (shells or layers). The mantle has five shells in the model, while the core is divided into an Inner Core (IC) and Outer Core (OC). There are also the ocean and two crust "thin" layers.

The change of $\rho_{\rm E}$ (N_e) from the mantle to the core, according to PREM, can well be approximated by a step function, the transition zone being relatively narrow (width ~ 100 km).

PREM: good/useful "Reference" model.

$\rho_{\rm E}^{\rm PREM}({\rm r}) = \rho_{\rm E}^{\rm PREM}(r)$, in particular. Used in practically all studies of ν tomography of the Earth.

Future: more sophisticated $\rho_{\rm E}({\rm r})$ suggested by geophysics/seismology can/should be used.

The Earth matter effects in the $\nu_{\mu(e)} \to \nu_{e(\mu)}$ ($\bar{\nu}_{\mu(e)} \to \bar{\nu}_{e(\mu)}$) oscillations depend on

$$V =^{+}_{(-)} \sqrt{2}\, G_{\mathsf{F}}\, N_e^{(E)}(r)$$

$$N_e^{(E)}(r) = \rho_{\mathsf{E}}(r)\, Y_e/m_{\mathsf{N}},$$

Y_e **- electron fraction number (or Z/A factor).**

For isotopically symmetric matter $Y_e = 0.5$.

Earth core composition models: $Y_e^c = 0.466 - 0.471$.

Earth mantle composition models: $Y_e^{man} = 0.490 - 0.496$.

However, varying Y_e^c and Y_e^{man} in the indicated respective intervals has no effect on the results on the $\bar{\rho}_{\mathsf{uman}}$, $\bar{\rho}_{\mathsf{lman}}$, $\bar{\rho}_{\mathsf{man}}$, $\bar{\rho}_{\mathsf{C}}$ $\bar{\rho}_{\mathsf{OC}}$, $\bar{\rho}_{\mathsf{IC}}$ determination.

Determining the composition of, e.g., the OC or IC is technically a very different problem with respect to determining $\bar{\rho}_{\mathsf{man}}$, $\bar{\rho}_{\mathsf{C}}$ $\bar{\rho}_{\mathsf{OC}}$, $\bar{\rho}_{\mathsf{IC}}$: does not require varying $\bar{\rho}_{\mathsf{i}}$ in the study.

Conclusion.

The neutrino tomography of the Earth is a promissing powerful alternative method of obtaining valuable information about the Earth interior. It is still in a stage of development. The neutrino tomography of the Earth can improve, or even push the boundaries of, our understanding of the Earth interior, which can have far-reaching fundamental implications. This can be done with existing and upcoming experiments IceCube-Deep Core, IceCube Upgrade, ORCA, Km3NeT, HK, DUNE, ... with atmospheric neutrinos. The physics potential of the neutrino tomography of the Earth should continue to be explored.

Supporting Slides

Articles on using atmospheric neutrinos for neutrino tomography of the Earth.

– M. C. Gonzalez-Garcia, F. Halzen, M. Maltoni and H. K. M. Tanaka, "Radiography of earth's core and mantle with atmospheric neutrinos," Phys. Rev. Lett. **100** (2008) 061802 [arXiv:0711.0745 [hep-ph]] (absorption tomography).

– A. Donini, S. Palomares-Ruiz and J. Salvado, "Neutrino tomography of Earth," Nature Phys. **15** (2019) 37 [arXiv:1803.05901 [hep-ph]] (absorption tomography).

– S. K. Agarwalla, T. Li, O. Mena and S. Palomares-Ruiz, "Exploring the Earth matter effect with atmospheric neutrinos in ice," [arXiv:1212.2238 [hep-ph]] (IceCube/DeepCore, PINGU; EHSE, $M_\oplus$ and $I_\oplus$ constraints not accounted for).

– W. Winter, "Atmospheric Neutrino Oscillations for Earth Tomography," Nucl. Phys. B **908** (2016), 250-267 [arXiv:1511.05154 [hep-ph]] (PINGU, ORCA; 7 layers, densities in these layers varied independently; EHSE, $M_\oplus$ and $I_\oplus$ constraints not taken into account; systematic errors "optimistic" (ORCA)).

– C. Rott, A. Taketa and D. Bose, "Spectrometry of the Earth using Neutrino Oscillations," Sci. Rep. **5** (2015), 15225 [arXiv:1502.04930 [physics.geo-ph]] (composition).

– S. Bourret *et al.* [KM3NeT], "Neutrino oscillation tomography of the Earth with KM3NeT-ORCA," J. Phys. Conf. Ser. **888** (2017) 012114 [arXiv:1702.03723 [physics.ins-det]] (ORCA; systematic errors not accounted for).

– S. Bourret *et al.* [KM3NeT], "Neutrino oscillation tomography of the Earth with KM3NeT-ORCA," PoS **ICRC2017** (2018) 1020 (doi:10.22323/1.301.1020).

– S. Bourret *et al.* [KM3NeT], "Earth tomography with neutrinos in KM3NeT-ORCA," EPJ Web Conf. **207** (2019) 04008 (doi:10.1051/epjconf/201920704008).

– S. Bourret, J. Coelho, E. Kaminski and V. Van Elewyck, "Probing the Earth Core Composition with Neutrino Oscillation Tomography," PoS **ICRC2019** (2020), 1024 (doi:10.22323/1.358.1024)

– S. Bourret, J. Coelho, E. Kaminski and V. Van Elewyck, "Probing the Earth Core Composition with Neutrino Oscillation Tomography," PoS **ICRC2019** (2020), 1024 (doi:10.22323/1.358.1024).

– A. Kumar and S. K. Agarwalla, "Validating the Earth's core using atmospheric neutrinos with ICAL at INO," JHEP **08** (2021) 139 [arXiv:2104.11740 [hep-ph]].

– V. Van Elewyck, J. Coelho, E. Kaminski and L. Maderer, "Probing the earth's interior with neutrinos," Europhys. News **52** (2021) 19 (doi:10.1051/epn/2021103).

– K. J. Kelly, P. A. N. Machado, I. Martinez-Soler and Y. F. Perez-Gonzalez, "DUNE atmospheric neutrinos: Earth tomography," JHEP **05** (2022) 187 [arXiv:2110.00003 [hep-ph]].

– P. B. Denton and R. Pestes, "Neutrino oscillations through the Earth's core," Phys. Rev. D **104** (2021) 113007 [arXiv:2110.01148 [hep-ph]].

– F. Capozzi and S. T. Petcov, "Neutrino tomography of the Earth with ORCA detector," Eur. Phys. J. C **82** (2022) 461 [arXiv:2111.13048 [hep-ph]].

– L. Maderer, E. Kaminski, J. A. B. Coelho, S. Bourret and V. Van Elewyck, "Unveiling the outer core composition with neutrino oscillation tomography," Front. Earth Sci. **11** (2023), 1008396 [arXiv:2208.00532 [hep-ex]].

– A. K. Upadhyay, A. Kumar, S. K. Agarwalla and A. Dighe, "Locating the core-mantle boundary using oscillations of atmospheric neutrinos," JHEP **04** (2023) 068 [arXiv:2211.08688 [hep-ph]].

– S. T. Petcov, "Neutrino tomography of the earth: the earth total mass, moment of inertia and hydrostatic equilibrium constraints," Eur. Phys. J. C **84** (2024) 991; (E): arXiv:2406.13727v.2 [hep-ph]].

– C. Jesús-Valls, S. T. Petcov and J. Xia, "Neutrino Oscillation Tomography of the Earth with the Hyper-Kamiokande Detector," [arXiv:2411.12344 [hep-ex]].

– S. Chattopadhyay, J. Krishnamoorthi and A. K. Upadhyay, "Demonstrating the ability of IceCube DeepCore to probe Earth's interior with atmospheric neutrino oscillations," Eur. Phys. J. ST **234** (2025) 5055-5064 [arXiv:2502.18995 [hep-ph]].

– J. Krishnamoorthi *et al.*, "Probing Earth's core using atmospheric neutrino oscillations in the presence of NSI at INO-ICAL," JHEP **10** (2025) 213 [arXiv:2507.02167 [hep-ph]].

– R. Abbasi *et al.* [IceCube Collaboration], "Estimating the sensitivity of the IceCube Upgrade to probe the interior of the Earth using atmospheric neutrino oscillations," [arXiv:2608.06543 [hep-ex]].

– S. K. Agarwalla *et al.*., "Deep Earth imaging through neutrino and seismic tomography," [arXiv:2608.15231 [hep-ex]].

Early studies:

– S. Choubey, P. Ghoshal and S.T.P., studies performed in the period 2008 - 2011 (HK, LAr), unpublished.

– S. Choubey and S.T.P., studies performed in 2014 (PINGU), unpublished.

(The list probably is not complete.)